

**SINGLE- AND MULTIPLE-STAGE CASCADED VAPOR COMPRESSION
REFRIGERATION FOR ELECTRONICS COOLING**

A Thesis
Presented to
The Academic Faculty

by

Charles Lee Coggins

In Partial Fulfillment
of the Requirements for the Degree
Master of Science in the
George W. Woodruff School of Mechanical Engineering

Georgia Institute of Technology
August 2007

**SINGLE- AND MULTIPLE-STAGE CASCADED VAPOR COMPRESSION
REFRIGERATION FOR ELECTRONICS COOLING**

Approved by:

Dr. Yogendra Joshi, Advisor
School of Mechanical Engineering
Georgia Institute of Technology

Dr. Andrei Fedorov, Co-advisor
School of Mechanical Engineering
Georgia Institute of Technology

Dr. Paul Kohl
School of Chemical and Biomolecular Engineering
Georgia Institute of Technology

Date Approved: May 1, 2007

*À ma chérie, Céline.
Merci de m'avoir soutenu.*

ACKNOWLEDGEMENTS

I would like to thank my advisors, Dr. Yogendra Joshi and Dr. Andrei Fedorov, for their direction, support, and patience during this research. I would also like to thank Dr. Paul Kohl for his strategic guidance and support as a member of my thesis committee. I would like to thank Dr. David Gerlach for serving as my mentor and reminding me of the joy of engineering. I would like to thank the members of the Microelectronics and Emerging Technologies Thermal Laboratory, in particular Dr. Yoon Jo Kim and Shivesh Suman, for their advice and our fruitful interactions. I would like to thank the School of Mechanical Engineering administrative staff for helping me with everything from enrollment to graduation, and the machine shop personnel for advising me on how to fabricate components for my experiment. I would like to thank my parents and grandparents for drawing from their own experiences to give me needed advice. Finally, I would like to thank the Interconnect Focus Center for funding my project.

TABLE OF CONTENTS

	Page
ACKNOWLEDGEMENTS	iv
LIST OF TABLES	viii
LIST OF FIGURES	ix
NOMENCLATURE	xii
SUMMARY	xv
<u>CHAPTER</u>	
1 BACKGROUND	1
1.1 Introduction	1
1.2 Literature Review	3
1.2.1 Vapor Compression Refrigeration in Electronics Cooling	3
1.2.2 Scaling of Vapor Compression Refrigeration Systems	5
1.3 Scope of Thesis	6
2 SCALING OF SINGLE- AND MULTIPLE-STAGE VCR SYSTEMS FOR ELECTRONICS COOLING	7
2.1 Concept of Scaling Analysis	7
2.2 Thermodynamic Analysis	7
2.2.1 Air-Cooled Condenser	9
2.2.2 Expansion Device	10
2.2.3 Evaporator	11
2.2.4 Compressor	11
2.2.5 Energy and Rate Analysis	12
2.2.6 Adding Additional Stages	12
2.2.7 Implications of Thermodynamic Analysis	14
2.3 Choice of Refrigerants	14

2.4 Predicting the Volume of Individual Components	16
2.4.1 Compressor	16
2.4.2 Heat Exchangers	18
2.4.3 Piping, Expansion Device, and Insulation	19
2.5 Comparing the Volumes of Individual Components	20
3 DEMONSTRATION OF A COMPACT, TWO-STAGE CASCADED VCR SYSTEM	23
3.1 System Design	23
3.2 Refrigeration Flow Loop	24
3.2.1 Compressor	25
3.2.2 Inter-stage Heat Exchanger	29
3.2.3 Low Stage Evaporator	30
3.2.4 Expansion Device	30
3.2.5 Air-Cooled Condenser	31
3.2.6 Miscellaneous Equipment	32
3.3 Test Procedure	33
3.4 Experimental Uncertainties	33
4 RESULTS AND DISCUSSION	35
4.1 Performance of the Two-Stage Cascaded VCR System	35
4.2 Comparison of the Experimental Results and the Thermodynamic Model	36
4.3 Comparison of the Scaling Analysis Results and Actual VCR Systems	38
5 CLOSING	42
APPENDIX A: EES Code for Scaling Analysis	44
APPENDIX B: VCR System Survey	56
APPENDIX C: Design of Two-Stage Cascaded VCR System using Converted Air Compressors	63
C.1 System Design Concept	63

C.2 Compressor Design and Fabrication	65
C.3 Changes in Refrigeration Flow Loop	74
C.4 Test Procedure	76
C.5 Experimental Uncertainties	76
C.6 Performance of Compressor	76
APPENDIX D: SolidWorks Drawings of Components for Converted Air Compressors	77
REFERENCES	79

LIST OF TABLES

	Page
Table 1.1: VCR systems designed electronics cooling.	5
Table 2.1: Predicted chip throughput enhancement for sub-ambient operation, compared with operation at 350 K ($3\sigma = 110$ mV).	15
Table 3.1: Initial compressor requirements determined from thermodynamic model.	23
Table 3.2: Performance of Danfoss BD80F operating at 4400 RPM with R134a ($T_{condenser} = 54.4^{\circ}\text{C}$; $T_{ambient} = 32^{\circ}\text{C}$; no subcooling).	26
Table 3.3: Capillary tube information.	30
Table 4.1: Test results of the two-stage cascaded VCR system.	35
Table 4.2: Temperature measurements from the two-stage cascaded VCR system (no heat load).	35
Table 4.3: Pressure measurements from the two-stage cascaded VCR system (no heat load).	36
Table 4.4: Single-Stage VCR Systems.	39
Table 4.5: Two-Stage VCR Systems.	39
Table A.1: EES Look-up Chart for j_H .	45
Table A.2: EES Look-up Chart for NTU.	45
Table C.1: Motor performance chart.	67
Table C.2: Comparison of new design and first experimental system.	68

LIST OF FIGURES

	Page
Figure 1.1: Increase in microprocessor performance due to lower temperature.	2
Figure 1.2: Cost over 5 years to cool a 100 W microprocessor.	3
Figure 2.1: An idealized, single-stage VCR system.	8
Figure 2.2: A two-stage cascaded VCR system.	9
Figure 2.3: Comparing the COP of idealized and real VCR systems ($T_{ambient} = 300$ K; $T_{evaporator} = 250$ K; all stages use R134a).	13
Figure 2.4: Comparing the COP of idealized and real VCR systems ($T_{ambient} = 300$ K; $T_{evaporator} = 173$ K; all stages use R134a).	14
Figure 2.5: Chip throughput per power consumption for sub-ambient cooling ($T_{ambient} =$ 300 K).	15
Figure 2.6: Comparing the volume of the compressor motor and displacement.	17
Figure 2.7: Comparing the volume of the individual components of a system with an evaporator heat load of 100 W.	20
Figure 2.8: Comparing the volume of the individual components of a system with an evaporator heat load of 200 W.	21
Figure 2.9: Comparing the volume of the individual components for a system with an evaporator heat load of 100 W and an ambient temperature of 323 K.	22
Figure 3.1: Refrigeration flow loop for a two-stage cascaded VCR system.	24
Figure 3.2: Two-stage cascaded VCR system developed in the study.	25
Figure 3.3: Danfoss BD80F used for the low stage compressor.	25
Figure 3.4: Compressor map of the Danfoss BD80F with R508b.	28
Figure 3.5: Compressor map of the Danfoss NF11FX with R404A.	28
Figure 3.6: Danfoss NF11FX used for the high stage compressor.	29
Figure 3.7: Inter-stage heat exchanger used in the system.	29
Figure 3.8: Inside the evacuated chamber housing the evaporator.	31

Figure 3.9: Air-cooled condenser and fan used on the high stage.	31
Figure 3.10: The bench-top experiment.	32
Figure 4.1: Thermodynamic Model vs. Actual Performance (no heat load).	37
Figure 4.2 Comparing the predicted total system volume (compressor and condenser) with actual systems.	39
Figure 4.3: Comparing the predicted compressor volumes with compressors of actual systems.	40
Figure 4.4: Comparing the predicted condenser volumes with condensers of actual systems.	40
Figure 4.5: Comparing complete systems with different refrigerant combinations.	41
Figure A.1: Flowchart for Scaling Analysis program.	44
Figure A.2: EES Diagram Window for Scaling Analysis program.	45
Figure B.1: The VapoChill SE.	56
Figure B.2: The VapoChill XE.	57
Figure B.3: The VapoChill XE II.	58
Figure B.4: The VapoChill Light Speed.	59
Figure B.5: The Prometeia Mach II GT.	60
Figure B.6: The two-stage cascaded VCR system used to test compact evaporators.	61
Figure B.7: The two-stage cascaded VCR system developed in this study.	62
Figure C.1: A small hermetic compressor, dismantled.	64
Figure C.2: Proposed layout of a two-stage cascaded VCR system with one motor.	65
Figure C.3: Schematic of the proposed two-stage cascaded VCR.	65
Figure C.4: Two inexpensive, commercially available, tire inflators.	66
Figure C.5: Small air compressor manufactured by the COIDO Corporation.	66
Figure C.6: Permanent magnet DC motor selected to drive the compressor.	67
Figure C.7: Air compressor with additional components required to convert it into a compressor suitable for refrigerants.	69
Figure C.8: Crank shaft with flexible coupling, bearings, rotating seals, and gear.	69

Figure C.9: Torque vs. Angle curve for compressor operating with R404A.	70
Figure C.10: Torque vs. Angle curve for compressor operating with R508b.	71
Figure C.11: Plot of motor speed versus motor torque.	72
Figure C.12: Predicted performance for the compressor using R508b.	73
Figure C.13: Predicted performance for the compressor using R404A.	73
Figure C.14: Gear train design.	74
Figure C.15: Compressor, Condenser, Evaporator Housing, and mass flow meter.	75
Figure C.16: The bench-top experiment for testing the compressor.	75
Figure D.1: SolidWorks drawing of brass power transmission hub.	77
Figure D.2: SolidWorks drawing of crankcase plug.	78
Figure D.3: SolidWorks drawing of compressor intake manifold.	78

NOMENCLATURE

Abbreviations

COP	coefficient of performance
VCR	vapor compression refrigeration

Symbols

A_n	gas-side heat transfer surface area (m^2)
C	compressor effective clearance volume ratio
f	frequency of compressor cycles (s^{-1})
h	enthalpy (Jkg^{-1})
k	polytropic coefficient
\dot{m}	mass flow rate of refrigerant (kgs^{-1})
P	pressure (bar)
P_d	motor power density (Wm^{-3})
\dot{Q}_{in}	heat input (W)
q_{in}	specific heat input (Jkg^{-1})
s	entropy ($JK^{-1}kg^{-1}$)
T	temperature (K or $^{\circ}C$)
T	torque (lbf-in or Nm)
$V_{compressor}$	total volume of compressor (m^3)
$V_{condenser}$	volume of air-cooled condenser, minus fan (m^3)
$V_{displacement}$	volume of compressor displacement (m^3)

V_{motor}	volume of compressor motor (m^3)
\dot{W}_{in}	power input to compressor (W)
w_{in}	specific work input to compressor (Jkg^{-1})
x	quality
α	heat transfer surface area per total heat exchanger volume (m^2m^{-3})
ε	heat exchanger effectiveness
η_v	volumetric efficiency of compressor
v_{in}	specific volume of refrigerant at compressor inlet (m^3kg^{-1})
$v_{v,sat,R134a}$	specific volume saturated vapor R134a (m^3kg^{-1})

Subscripts

1	state point 1: exit of condenser two-phase region
2	state point 2: exit of condenser sub-cooled region
3	state point 3: exit of expansion device
4	state point 4: exit of evaporator
5	state point 5: exit of compressor
6	state point 6: exit of condenser desuper-heated region
<i>evap</i>	evaporator or evaporating
<i>cond</i>	condenser or condensing
<i>compressed</i>	exit of compressor
<i>subcooled</i>	exit of condenser sub-cooled region
<i>expanded</i>	exit of expansion device
<i>superheat</i>	exit of evaporator (if refrigerant is superheated)
<i>discharge</i>	exit of compressor

<i>suction</i>	inlet of compressor
<i>h,i</i>	inlet of hot side of heat exchanger
<i>c,i</i>	inlet of cold side of heat exchanger
<i>AT</i>	approach temperature
<i>DT</i>	temperature difference
<i>chip</i>	chip/microprocessor, or referring to surface of heater block

SUMMARY

The International Technology Roadmap for Semiconductors (ITRS) predicts that microprocessor power consumption will continue to increase in the foreseeable future. It is also well known that microprocessor performance can be improved by lowering the junction temperature: recent analytical studies show that for a power limited chip, there is a non-linear scaling effect that offers a 4.3x performance enhancement at $-100\text{ }^{\circ}\text{C}$, compared to $85\text{ }^{\circ}\text{C}$ operation. Vapor Compression Refrigeration (VCR) is a sufficiently compact, low cost, and power efficient technology for reducing the junction temperature of microprocessors below ambient, while removing very high heat fluxes via phase change.

The current study includes a scaling analysis of single- and multiple-stage VCR systems for electronics cooling and an experimental investigation of small-scale, two-stage cascaded VCR systems. In the scaling analysis, a method for estimating the size of single- and multiple-stage VCR systems is described, and the resulting trends are presented. The compressor and air-cooled condenser are shown to be by far the largest components of the system, dwarfing the evaporator, expansion device, and inter-stage heat exchanger. For systems utilizing off-the-shelf components and removing up to 200 W at evaporator temperatures as low as 173 K, compressor size dominates the system and scales with the compressor's motor. The air-cooled condenser is the second largest component, and its size is constrained by the air-side heat transfer coefficient. In the experimental work, a two-stage cascaded VCR system with a total volume of 60000 cm^3 is demonstrated that can remove 40 W at $-61\text{ }^{\circ}\text{C}$.

CHAPTER 1

BACKGROUND

1.1 Introduction

Over the past decade, the performance of laptop, desktop, and server computers has dramatically improved due to miniaturization of Complementary Metal Oxide Semiconductor (CMOS) technology and faster clock rates. However, in order to meet this enhanced functionality, power consumption, and therefore heat dissipation rates, have also rapidly increased. The International Technology Roadmap for Semiconductors (ITRS) predicts that the maximum power of high performance microprocessors will reach 198 W by 2008 [1], making it increasingly difficult, or even impossible, to meet thermal management demands with either conventional air-cooling or non-chilled liquid cooling [2].

It has also long been known that microprocessor performance can be improved by lowering the junction temperature. Recently, Naeemi and Meindl [3] showed that, due to a decrease in leakage current at low temperature operation, a CMOS chip has the potential of achieving a 4.3x performance enhancement at -100 °C, compared to 85 °C operation, when operated in a power limited mode. This is predicted by Equation 1.1 and shown in Figure 1.1.

$$f = \frac{T_{chip}^{-\alpha}}{358K} \quad \text{for } \alpha = 0.5, 0.75, 2 \quad (1.1)$$

In addition to enhanced chip throughput, sub-ambient cooling offers orders of magnitude improvement in reliability [4].

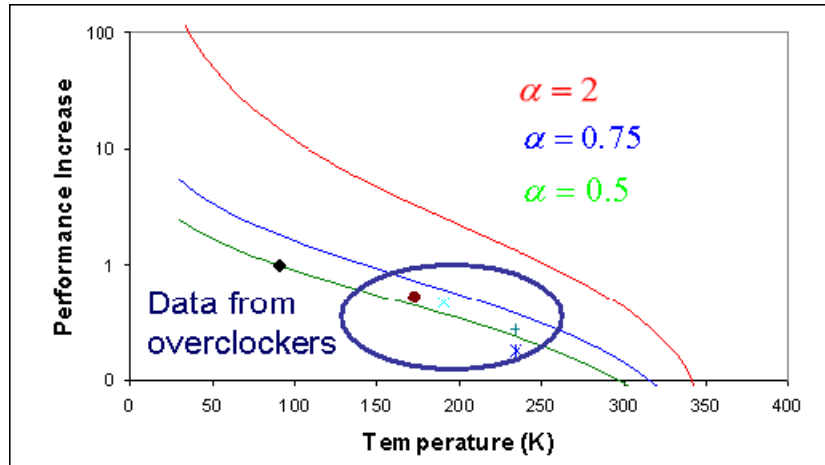


Figure 1.1: Increase in microprocessor performance due to lower temperature [5].

Vapor Compression Refrigeration (VCR) offers a practical means for removing large amounts of heat at sub-ambient temperatures and is a compelling technology to consider for increasing the performance and reliability of electronics [4]. After decades of development and extensive use in a wide range of applications, VCR systems have become very reliable and can be made sufficiently compact to fit in a desktop tower or a server rack. In fact, VCR is already used to directly cool computer and telecommunications equipment in some high performance applications [6]. IBM was the first to use refrigeration on high-end computing systems and developed a system that could remove 1050 W at 35 °C [4]. There is also a niche market for single-stage VCR systems designed to fit inside standard desktop towers. Two companies, for example, currently sell personal computer cooling systems using off-the-shelf VCR technology that can dissipate 200 W at -30 °C [7,8].

To reach temperatures lower than about -50 °C, two or more single-stage VCR systems can be coupled in a cascade. Recently, a two-stage cascaded VCR system was demonstrated that could remove 100 Wcm⁻² at a chip temperature of -63 °C [5], and amateur "overclocking" enthusiasts have demonstrated VCR systems with two or more stages that have achieved evaporator temperatures below -100 °C [9]. Such systems cost orders of magnitude below the alternatives, such as complex cryogenic systems or open cooling cycles utilizing cryogenic fluids [4,5].

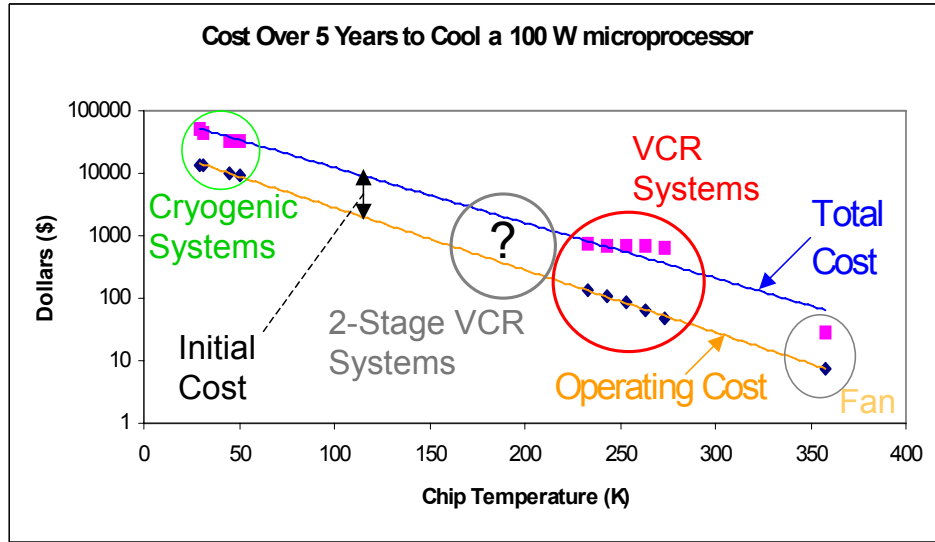


Figure 1.2: Cost over 5 years to cool a 100 W microprocessor [5].

While VCR systems offer an attractive option for operating high-performance computers and large servers at sub-ambient temperatures, their size is still a concern to packaging engineers. Until VCR systems can be made compact enough to easily integrate into electronics packages, widespread application of refrigeration in electronic cooling will remain limited [2].

1.2 Literature Review

1.2.1 Vapor Compression Refrigeration in Electronics Cooling

Several recent studies have described the design, modeling, and construction of small VCR systems for microprocessors. In 1997, IBM shipped the S/390 G4 CMOS system, the first high-end system to use refrigeration [4]. With two Modular Refrigeration Units (MRU) that fit inside a 6 U package (26.7 cm), the system was designed to dissipate 1050 W at 35 °C from a G4 multichip module. The COP of the system varied from 2 to 3 depending on the environmental conditions. Ellsworth *et al.* [10] designed cold plates to interface the VCR system with the chips and dealt with condensation through the use of insulation, desiccants, and strategically placed heaters. While the authors acknowledged that refrigeration is more costly and uses more power than more

basic thermal management techniques, these disadvantages were offset by gains in microprocessor performance and reliability for the targeted high-end systems.

Researchers have explored designs to reduce the size of VCR systems in order to make them more attractive for electronics packaging. Chow *et al.* [11] presented a preliminary design and analysis of a meso-scale refrigerator to be created from layers of silicon wafers bonded together and fabricated through the techniques of microelectronics. The system was designed to remove 32 W at 12 °C, with a COP of 3.34, using a centrifugal compressor driven by an electrostatically actuated, pancake-shaped motor. Heydari [12] evaluated a CPU spot cooling refrigeration system and developed a thermodynamic model describing the performance of the cycle. The system was designed to reduce the 86 °C chip junction temperature down to 20 °C using a miniature, oil-less, linear reciprocating compressor that could operate at an estimated COP of 3.0. Phelan *et al.* [13] explored the possibility of developing a mesoscale VCR system less than ~5 cm in size that could be integrated into high power microelectronics packaging. While the authors determined that heat loads of up to 300 W could be dissipated at 5 °C using commercially available scroll compressors, the compressor itself could not fit inside the desired 5 cm package. Researchers from Intel [14] recently designed and built a VCR system small enough to fit inside of a notebook computer, removing 50 W at 50 °C using isobutene as a refrigerant. Also recently, a two-stage cascaded R134a/R508b VCR system was developed to perform two-phase flow boiling experiments with compact, copper-made evaporators [5]. Utilizing an evaporator with a micromilled, alternating pin fin geometry, the system was shown to dissipate 100 W from a 1 cm² chip at -62.6 °C. However, this system was not optimized for size. These systems are summarized in Table 1.1.

Table 1.1: VCR systems designed for electronics cooling.

	Schmidt and Notohardjono [4]	Asetek, Inc. [7]	Chow <i>et al.</i> [11]	Heydari [12]	Phelan <i>et al.</i> [13]	Mongia <i>et al.</i> [14]	Wadell [5]
Heat Load [W]	525	200	32	–	100-300	50	100
T_{evaporator} [°C]	15-35	-33	12	20	5	50	-62.6
T_{condensing} (T_{ambient}) [°C]	–	–	(45)	60	55	90 (50)	(25)
Flow Rate [gmin⁻¹]	–	–	16.3	–	–	12.5 cm ³ s ⁻¹	70
Number of Stages	1	1	1	1	1	1	2
System Volume	27x27x71 cm	21x21x49 cm	Meso-scale	–	~15x5x5 cm	Notebook Computer	~0.4 m ³
System Mass	27 kg	15 kg	–	–	–	–	–
Refrigerant	R134a	R507A	R134a	R134a	R134a	R600a (Isobutane)	R134a / R508b
COP	2-3	–	3.34	3.0	~3	>2.25	–
Compressor Type(s)	DC Rotary	AC Reciprocating	Centrifugal	Linear	Scroll	DC Reciprocating	2 x AC Reciprocating

1.2.2 Scaling of Vapor Compression Refrigeration Systems

There have been several studies regarding both small scale single-stage VCR systems for electronics cooling and the optimization of two-stage VCR systems. The studies on single-stage systems developed thermodynamic models for the components of small VCR systems [12], optimized heat exchanger size [15], surveyed available compressor technologies appropriate for small systems [13], and considered the difficulty of miniaturizing VCR systems due to the effect decreasing system scale has on each component's entropy generation [16]. Recent studies on two-stage cascaded VCR systems have sought to determine the optimal intermediate temperature or pressure that would maximize the overall system's coefficient of performance (COP) of cooling [17,18]. However, these studies address neither overall system size, nor scaling issues as a function of cooling capacity and evaporator temperature.

1.3 Scope of Thesis

In Chapter 2, a method for predicting the size of single- and multiple-stage VCR systems is described. This method is used to develop an analytical tool that allows a systems designer to determine if a VCR system is appropriate for a particular application. The analysis allows comparing system size as a function of cooling capacity and evaporator temperature, as well as the sizes of single- and multiple- stage VCR systems.

Chapter 3 describes the development of a compact, two-stage cascaded vapor compression refrigeration system designed to interface with a high-performance microprocessor. The goal of this effort was to build a system that (a) can remove 100 Wcm⁻² at a low chip operating temperature (-70 °C); (b) is small enough for integration with a high performance computer (15x18x30 cm or ~8100 cm³); (c) has a low total cost (initial cost plus operating cost); and (d) is reliable. Because of the requirement for low system cost, this problem was approached by using off-the-shelf parts and improved component matching.

Chapter 4 presents the results of the scaling analysis and compares them with actual single- and two-stage VCR systems, including the system developed for this study. The trends resulting from the analysis illuminate the bottlenecks that limit further system miniaturization.

CHAPTER 2

SCALING OF SINGLE- AND MULTIPLE-STAGE VCR SYSTEMS FOR ELECTRONICS COOLING

2.1 Concept of Scaling Analysis

This scaling analysis considers single-stage and multiple-stage cascaded VCR systems using off-the-shelf components. The objective is to develop an analytical tool that allows a systems designer to determine if a VCR system is appropriate for a particular application. The investigation begins with the thermodynamic analysis of a simple, single-stage VCR system. The addition of a second stage is considered next, followed by the addition of more stages. Heat transfer analysis, along with the thermodynamic rate analysis, are used to predict the volume of each component in the VCR system.

2.2 Thermodynamic Analysis

A simple, single-stage VCR system consists of a compressor, air-cooled condenser, expansion device, and evaporator. In electronics cooling applications, the refrigeration system must interface with the microprocessor or other high power component by means of a high heat flux, low temperature, compact, cold plate evaporator. The minimum temperature and the maximum heat load that can be removed by the evaporator are determined by the system's components: the power of the compressor; the air-side heat transfer coefficient of the condenser; the ambient temperature; the working fluid; etc.

This scaling investigation begins with the thermodynamic analysis of an idealized VCR system. In this simplified system, shown in Figure 2.1, the compressor is assumed to be isentropic, the heat exchangers are isobaric, and the expansion device is isenthalpic. Pressure losses in connecting pipes are neglected, and heat transfer with the surroundings only occurs in the air-cooled condenser [18].

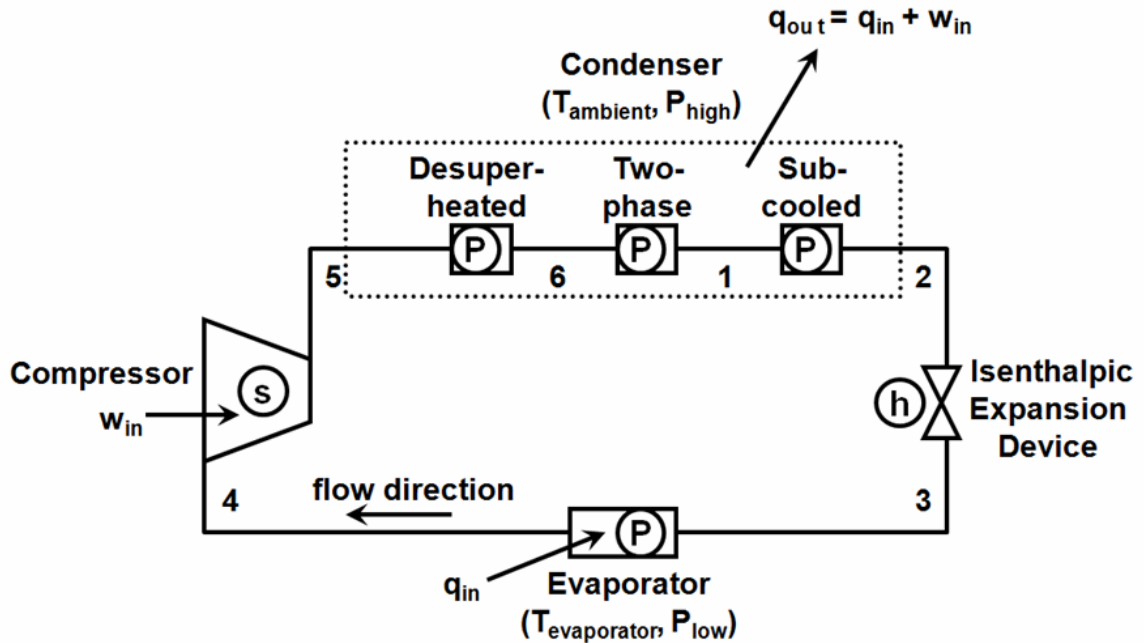


Figure 2.1: An idealized, single-stage VCR system.

A two-stage cascaded VCR system, shown in Figure 2.2, can achieve a lower evaporator temperature by configuring two single-stage systems in series. The evaporator of the high stage removes the heat from the condensing refrigerant in the low stage, allowing the low stage evaporator to reach an even lower temperature. The component that interfaces the two stages is the inter-stage heat exchanger, sometimes referred to as a “cascade condenser.” An air-cooled condenser is still used on the high stage, where all of the heat generated and transported by the system is ultimately dissipated to the ambient, typically via forced convection. Additional stages can be added in between the high and low stages, each interfaced to the next through an inter-stage heat exchanger, resulting in a multi-stage system.

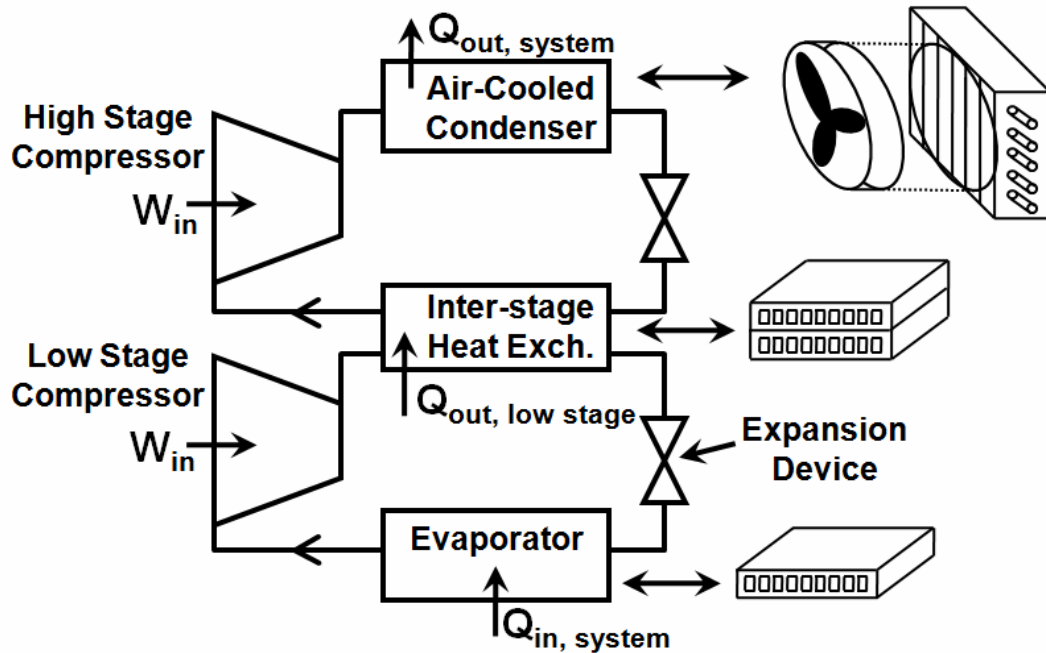


Figure 2.2: A two-stage cascaded VCR system.

2.2.1 Air-Cooled Condenser

The condenser is divided into three zones of desuperheated, two-phase, and subcooled regions [19], and the refrigerant condenses at a negligible temperature difference from the ambient.

2.2.1.1 Desuperheated Region

The high pressure of the system is set so that the condensing temperature is above the ambient temperature. In the idealized system, the temperature difference (T_{DT}) between the ambient ($T_{ambient}$) and the saturated vapor exiting the desuperheated region (T_6) is 0.00001 K, while in the real system, it is 5 K.

$$x_6 = 1 \quad (2.1)$$

$$T_6 = T_{DT} + T_{ambient} \quad (2.2)$$

Once two properties at the state point are known, the remaining properties (pressure, enthalpy, entropy, volume, etc.) can be determined. The pressure at this point will be the highest pressure (P_{high}) in the cycle.

$$P_6 = P_{high} = P(T_6, x_6) \quad (2.3)$$

$$h_6 = h(T_6, x_6) \quad (2.4)$$

2.2.1.2 Condensing Region (Two-Phase Mixture)

The refrigerant will exit the condensing region as a saturated liquid. The pressure will remain P_{high} .

$$x_1 = 0 \quad (2.5)$$

$$P_1 = P_{high} \quad (2.6)$$

2.2.1.3 Subcooled Region (Subcooled Liquid)

In the idealized system, the condensed refrigerant is subcooled to the ambient temperature, so the approach temperature is zero ($T_{AT} = 0K$). In the more realistic system, the refrigerant is subcooled to 3 K below the condensing temperature

$$T_{AT} = T_{DT} - 3K = 2K \quad (2.7)$$

$$T_2 = T_{ambient} + T_{AT} \quad (2.8)$$

The pressure remains the high system pressure

$$P_2 = P_{high} \quad (2.9)$$

2.2.2 Expansion Device

Next, the refrigerant is throttled in an expansion device. This expansion is assumed to be isenthalpic

$$h_3 = h_2 \quad (2.10)$$

The expansion device exit temperature will be the same as the desired evaporator temperature, which is a system input

$$T_3 = T_{evaporator} \quad (2.11)$$

The quality at the exit of the expansion device will be between 0 and 1.

2.2.3 Evaporator

The low pressure, low temperature, two-phase mixture enters the evaporator and boils until it exits the evaporator as a saturated vapor. The evaporator pressure (P_4), and also thus the low pressure of the cycle (P_{low}), is the saturation pressure at the desired evaporator temperature

$$x_4 = 1 \quad (2.12)$$

$$P_4 = P_{low} = P(T_4, x_4) \quad (2.13)$$

2.2.4 Compressor

The low temperature, low pressure, saturated refrigerant vapor enters the compressor to be compressed to a superheated gas at P_{high} .

$$P_5 = P_{high} \quad (2.14)$$

The enthalpy for isentropic compression can be determined

$$s_{s,5} = s_4 \quad (2.15)$$

$$h_{s,5} = h(P_5, s_{s,5}) \quad (2.16)$$

To find the actual enthalpy, a user defined compressor isentropic efficiency ($\eta_{compressor}$) is selected, depending on the type of compressor, and

$$h_5 = h_4 + \frac{h_{s,5} - h_4}{\eta_{compressor}} \quad (2.17)$$

The temperature at the exit of the compressor is

$$T_5 = T(P_{high}, h_5) \quad (2.18)$$

2.2.5 Energy and Rate Analysis

Now that the enthalpy is known for each state point, it is possible to determine the required specific work input (w_{in}) and the specific heat input (q_{in})

$$w_{in} = h_5 - h_4 \quad (2.19)$$

$$q_{in} = h_4 - h_3 \quad (2.20)$$

The cycle coefficient of performance (COP) is the heat input divided by the actual work input

$$COP = \frac{q_{in}}{w_{in}} \quad (2.21)$$

The relative efficiency of a refrigeration cycle can be measured by comparing its COP with the Carnot COP, which is the highest COP that a refrigerator operating between a set of temperature limits, T_L and T_H , can have

$$COP_{Carnot} = \frac{1}{\frac{T_H}{T_L} - 1} = \frac{1}{\frac{T_{ambient}}{T_{evaporator}} - 1} \quad (2.22)$$

Finally, the required compressor mass flow rate (\dot{m}) can be determined with the user defined evaporator heat load (\dot{Q}_{in})

$$\dot{m} = \frac{\dot{Q}_{in}}{q_{in}} \quad (2.23)$$

2.2.6 Adding Additional Stages

If a second stage is added to the system, it is necessary to determine the point at which the stages should interface. Because the refrigerants, and therefore the saturation pressures, in each stage may be different, temperature is used to select an interface point. The intermediate temperature is determined numerically, via iterative procedure, to maximize overall system COP [16]. As additional stages are added to an idealized system, the system COP increases to approach an asymptotic maximum below the Carnot COP. Figures 2.3 and 2.4 show that a more realistic system, with a

compressor isentropic efficiency of 0.4 [20,21] and a heat exchanger overlap temperature of 5 K [18], will have a much lower COP than the idealized system. The COP of a realistic system will peak at one, two, or three stages, depending on the evaporator and ambient temperatures and the refrigerants used in each stage. The system COP will decrease as more stages are added due to the penalizing effect of the temperature overlap in the heat exchangers, as well as compressor inefficiencies.

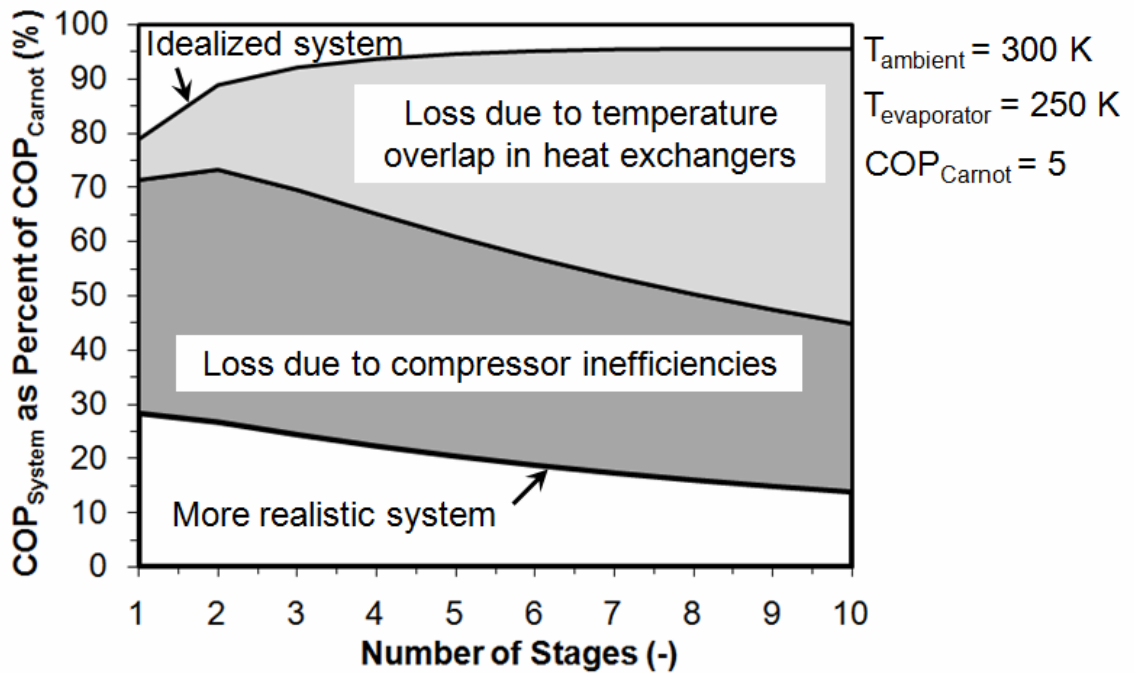


Figure 2.3: Comparing the COP of idealized and real VCR systems ($T_{\text{ambient}} = 300 \text{ K}$;

$T_{\text{evaporator}} = 250 \text{ K}$; all stages use R134a).

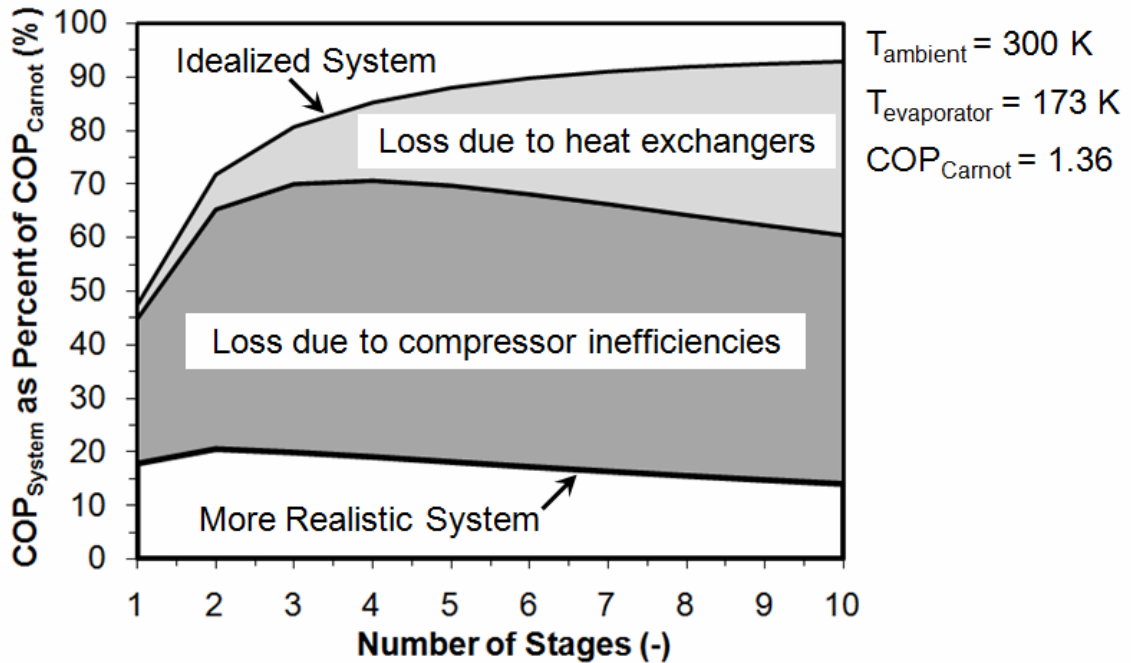


Figure 2.4: Comparing the COP of idealized and real VCR systems ($T_{ambient} = 300$ K; $T_{evaporator} = 173$ K; all stages use R134a).

Because more power is input into the refrigerant in order to reach lower temperatures, the temperature of the refrigerant exiting the compressor will increase as the temperature span of a single stage increases. Therefore, it may be necessary to break a large temperature difference into two or more stages. An evaporator temperature of 173 K, for example, might require 3 stages.

2.2.7 Implications of Thermodynamic Analysis

With energy costs rising, the importance of power efficiency in thermal management solutions has increased in recent years. Today's high performance computer systems are often compared by dividing the microprocessor performance, in million instructions per second (MIPS), by the total power input required to achieve this performance. Naeemi [22] predicted the performance enhancement due to sub-ambient temperature operation for microprocessors with constant leakage and active powers. Table 2.1 shows the predicted throughput enhancement for a microprocessor with a

transistor threshold voltage (V_{th}) variation (3σ) of 110 mV (predicted at the end of the ITRS) and chip powers at 20% of the plug power (P_{Plug}). Using these values, along with the COPs developed in the thermodynamic analysis for single- and multiple-stage VCR systems, Figure 2.5 shows the performance improvement per total power input for operating temperatures of 120 K to 300 K. Assuming an ambient temperature of 300 K, a single-stage VCR system could improve chip throughput per power consumption $\sim 1.7x$ at 240 K, compared to operation at 350 K. Likewise, a $\sim 2x$ improvement in chip throughput per power consumption can be expected at 200 K using a two-stage VCR system. Temperatures below 200 K might not be desirable from a power efficiency stand-point.

Table 2.1: Predicted chip throughput enhancement for sub-ambient operation, compared with operation at 350 K ($3\sigma = 110$ mV) [22].

Temperature [K]	120	140	160	180	200	220	240	260	280	300
MIPS/ MIPS@350K	5.54	4.94	4.00	3.31	3.02	2.56	2.04	1.78	1.56	1.38

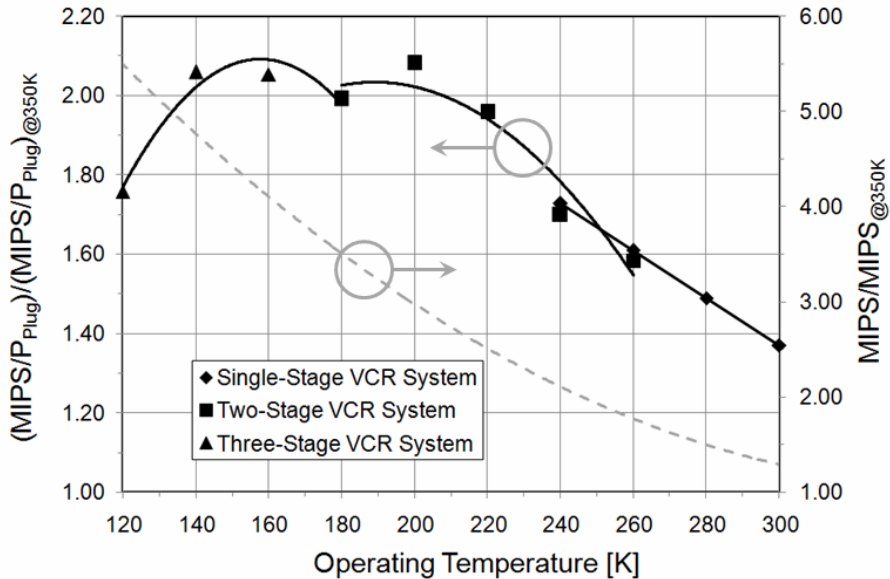


Figure 2.5: Chip throughput per power consumption for sub-ambient cooling ($T_{ambient} = 300$ K).

2.3 Choice of Refrigerants

In this analysis, the refrigerants R134a, R404A, R507A, and R508b are considered because they are commonly used in single- and multiple-stage VCR systems designed for electronics cooling. R134a, R404A, and R507A are used in single-stage systems and in the high stage of two-stage systems. Because of its low boiling point of 184.6 K at 1 bar, R508b is often used in the low stage of cascade systems [23]. A high stage is required to condense R508b below its critical temperature of 287.1 K. The thermodynamic properties of the refrigerants are calculated using the refrigeration property tables and routines included with EES [24].

2.4 Predicting the Volume of Individual Components

2.4.1 Compressor

In this analysis, off-the-shelf, electric, reciprocating compressors are considered because of their ruggedness, low cost, and availability. Such compressors are actuated by electric motors, and the motor size (V_{motor}) is estimated by using the work input (\dot{W}_{in}) calculated in the thermodynamic analysis and available power density (P_d) data for 4-pole, 3 phase induction motors [25]

$$P_d = 1.76\dot{W}_{in} + 208000 \quad (2.24)$$

$$V_{motor} = \frac{\dot{W}_{in}}{P_d} \quad (2.25)$$

The compressor's displacement volume ($V_{displacement}$) is estimated by using the mass flow rate and the inlet refrigerant volume (v_{in}) calculated in the thermodynamic analysis, and by assuming that the reciprocating compressor operates at a frequency (f) of 60 Hz and a volumetric efficiency (η_v) of 50% [13,21]

$$V_{displacement} = \frac{\dot{m}v_{in}}{f\eta_v} \quad (2.26)$$

When V_{motor} and $V_{displacement}$ are compared, as in Figure 2.6, it is clear that the motor defines the compressor size.

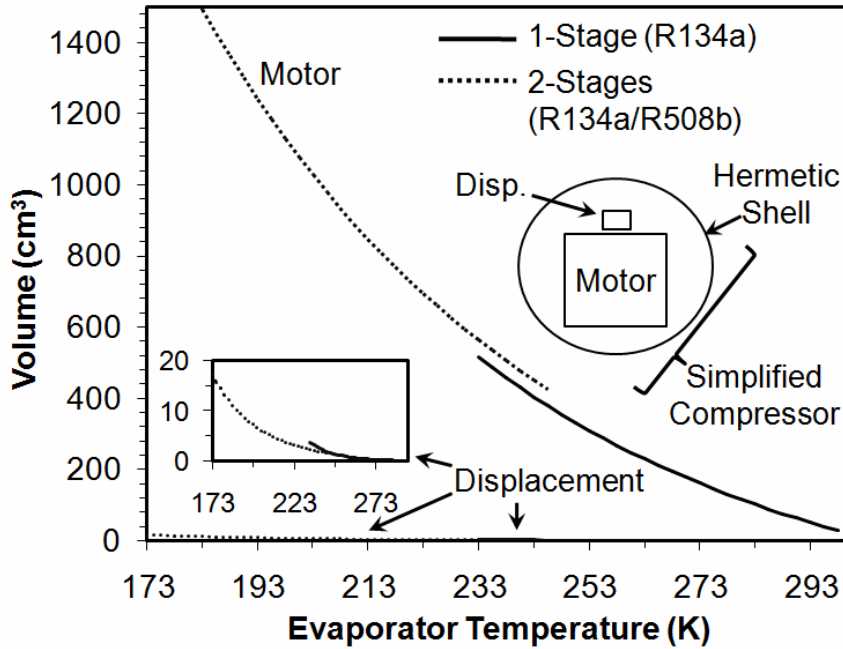


Figure 2.6: Comparing the volume of the compressor motor and displacement.

From dismantling several off-the-shelf reciprocating compressors, it was estimated that the volume of the hermetic shell enclosing the compressor ($V_{compressor}$) is typically 4-5 times larger than the motor:

$$V_{compressor} \cong 5V_{motor} \quad (2.27)$$

Besides ease of manufacture, the large shell allows room for the compressor motor, which is mounted on springs, to oscillate due to start-up and shut-down torque; allows oil pooled on the bottom of the shell to be sucked through the crankshaft and sprayed on the top of the shell to enhance lubrication and heat transfer; and allows the low pressure suction refrigerant to flow over and cool the motor before being compressed. It is quite possible that a reciprocating compressor, as well as other compressor technologies, such as rotary or scroll, could have a hermetic shell that fits more snugly around the compressor actuator.

2.4.2 Heat Exchangers

The sizes of the air-cooled condenser, evaporator, and inter-stage heat exchanger are each calculated using heat transfer analysis. It is assumed that the saturation temperature of the condensing fluid is 5 K above the evaporating fluid and there is 3 K of subcooling [18].

2.4.2.1 Air-Cooled Condenser

The air-cooled condenser is modeled as a circular tube, continuous fin heat exchanger with the heat transfer and flow characteristics of surface 8.0-3/8T from Kays and London [26]. A frontal area of 0.02 m² was selected, which is similar to the actual systems surveyed for this study. By using the effectiveness-NTU Method to determine the required gas-side heat transfer surface area (A_h), the required heat exchanger volume ($V_{condenser}$) can then be determined by dividing this value by the heat transfer surface area per total heat exchanger volume (α) [27]

$$V_{condenser} = \frac{A_h}{\alpha} \quad (2.28)$$

While more advanced condenser technology, such as extruded aluminum microchannels and louvered fins, is available, all of the actual systems surveyed for this study used condensers similar to the more simple design modeled here. The total volume of the air-cooled condenser also includes a fan, which is required to force air over the condensing coils. A fan is selected with dimensions of 12.7 cm x 12.7 cm x 3.8 cm that can provide an airflow of 167 CFM (0.0788 m³s⁻¹) in low-impedance.

2.4.2.2 Evaporator Cold Plate

The evaporator internal design optimizes heat transfer by increasing both the surface area convective heat transfer coefficient and the length of the refrigerant path. The size of the evaporator is estimated using the boiling heat transfer coefficient correlations developed by Lee and Mudawar [28] for R134a. This model assumes a uniform heat flux of 93.8 Wcm⁻², so the evaporator size is linearly proportional to amount

of heat removed. In addition, recent studies have shown that copper milled offset pin fins can achieve 100 Wcm^{-2} in evaporation of R508b [29].

2.4.2.3 Inter-stage Heat Exchanger

The inter-stage heat exchanger is designed as a microchannel evaporator coupled, via common heat transfer interface, with a microchannel condenser. The condensation heat transfer coefficient, calculated using the correlation of Akers *et al.* [30], is less than the boiling heat transfer coefficient, so the inter-stage heat exchanger volume is estimated by determining the surface area required to condense the refrigerant. A more recent correlation for condensation heat transfer coefficient, such as Bandhauer *et al.* [31], could be used, but it would not significantly change the results of this study. In the desuperheated and subcooled regions, the convection heat transfer is calculated for a single-phase gas and a single-phase liquid, respectively. The two-phase region is further discretized, and the heat transfer is calculated based on the quality of the refrigerant in each cell.

2.4.3 Piping, Expansion Device, and Insulation

The volumes of a VCR system's piping, expansion device, and insulation are not considered in this analysis. The volumes of copper tubing and simple expansion devices, such as capillary tube, are negligible when compared to the other components. The volume of insulation is more significant, especially at low temperatures. For example, at an evaporator temperature of 173 K, 3 cm of foam insulation would increase the evaporator volume from about $\sim 10 \text{ cm}^3$ to about $\sim 250 \text{ cm}^3$. The use of vacuum-jacketed insulation can minimize additional volume added to the system, but at the expense of significant cost increases and more difficult maintenance. In addition, any components operating at temperatures below the dew point must be appropriately insulated to avoid condensation or freezing of water on electronic components.

2.5 Comparing the Volumes of Individual Components

The sizes of the components were calculated for evaporator heat loads of 100-200 W, ambient temperatures of 300-323 K, and evaporator temperatures of 173-321 K. As seen in Figures 2.7 and 2.8, the compressor and air-cooled condenser are by far the largest components of the system, dwarfing the evaporator and inter-stage heat exchanger. For off-the-shelf systems removing up to 200 W of power, the air-cooled condenser is the largest component for evaporator temperatures above $\sim -15^\circ\text{C}$. The condenser size is constrained by the magnitude of the air-side heat transfer coefficient. For evaporator temperatures below $\sim -15^\circ\text{C}$, compressor size dominates the system and scales with the compressor's motor.

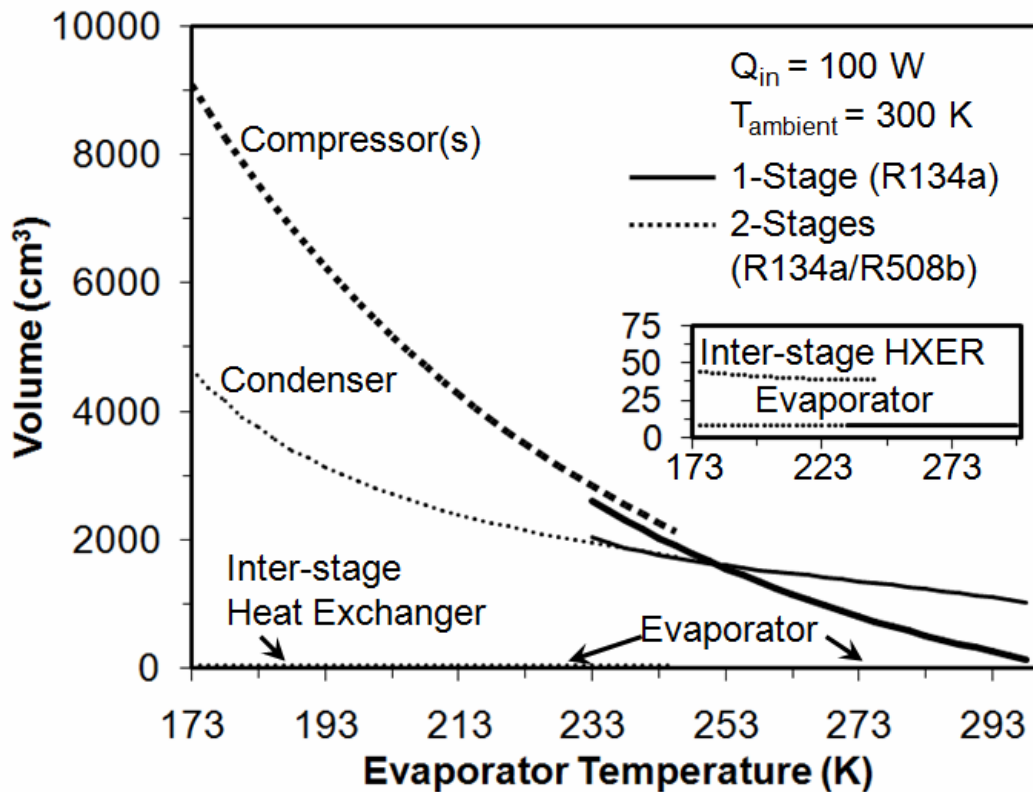


Figure 2.7: Comparing the volume of the individual components of a system with an evaporator heat load of 100 W.

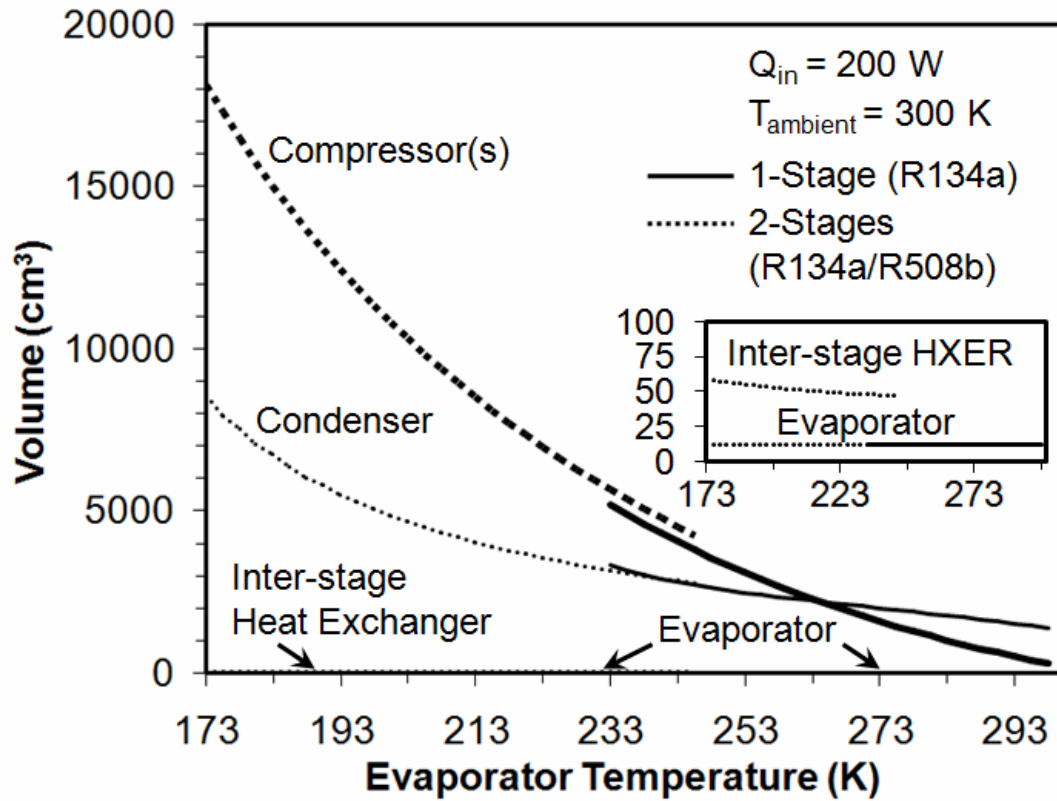


Figure 2.8: Comparing the volume of the individual components of a system with an evaporator heat load of 200 W.

When the ambient temperature is raised to 323 K, the graph shifts somewhat, as seen in Figure 2.9. The addition of a third stage lowers the high stage compressor discharge temperature, reducing the volume of the air-cooled condenser.

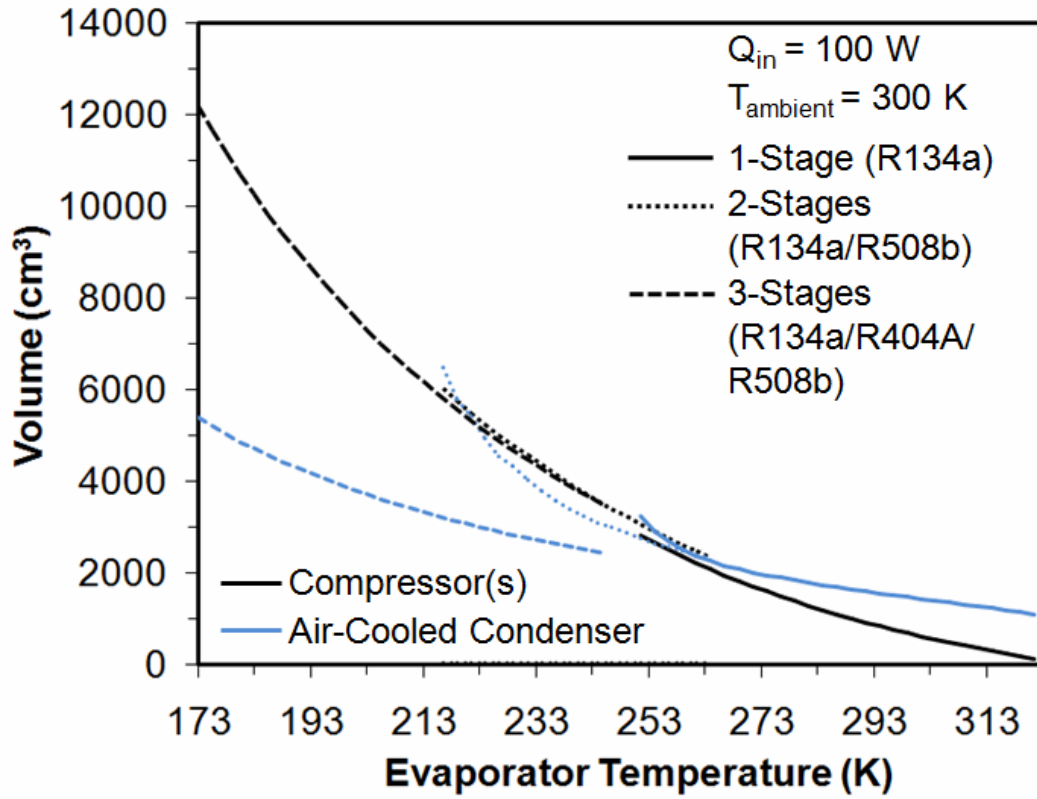


Figure 2.9: Comparing the volume of the individual components of a system with an evaporator heat load of 100 W and an ambient temperature of 323 K.

CHAPTER 3

DEMONSTRATION OF A COMPACT, TWO-STAGE CASCADED VCR SYSTEM

3.1 System Design

The purpose of this experimental work was to demonstrate that a two-stage cascaded VCR system could be built small enough to be integrated with a high performance desktop computer, and to validate the volume predictions developed in the scaling analysis. The cost of the system was minimized by using widely available, off-the-shelf components.

The development of the system began with the thermodynamic rate analysis described in Chapter 2. The system requirements developed using the analysis, shown in Table 3.1, were used to select two compressors, an air-cooled condenser, and an inter-stage heat exchanger. The compact evaporator and evacuated housing were retained from the reference [5]. R404A was chosen for the high stage refrigerant. R404A is a near-azeotropic blend of R125 / R143a / R134a with mass percentages of 44% / 52% / 4%. With a lower saturation temperature than R134a (-46.8 °C at 1 bar, versus -26.4 °C for R134a), R404A is well suited for low temperature applications. R508b, with a saturation temperature of -88.5 °C at 1 bar, is well suited for the low stage of cascaded systems.

Table 3.1: Initial compressor requirements determined from thermodynamic rate model.

	Refrigerant	Capacity [W]	Mass Flow Rate [kgs ⁻¹]	T _{evap} [°C]	T _{cond} (T _{amb}) [°C]	P _r
High Stage	R404A	190	0.001398	-26.4	57.4 (25)	5.5
Low Stage	R508b	100	0.000862	-70	11.4	5.3

3.2 Refrigeration Flow Loop

Figure 3.1 shows a schematic of the two-stage cascaded VCR system developed in this study. In addition to the four basic components of a VCR system, a few minor components were also used. A refrigerant receiver, located after each stage's condenser, ensured that only liquid refrigerant entered the expansion device, and served as a storage volume for refrigerant when the system was shut off. Following the receiver and a filter/drier, a metering needle valve and a capillary tube throttled the refrigerant. On the high stage, the capillary tube was wrapped around the suction line to create a liquid-suction heat exchanger which sub-cooled the liquid refrigerant entering the evaporator and boiled any remaining liquid refrigerant in the suction line.

Some other common components were not used in this system. An oil separator, which prevents oil from reaching the evaporator and potentially reducing the heat transferred to the refrigerant, was not used in this system. While an oil separator could improve system performance and reliability, the volume cost of this component out-weighed these benefits. For similar reasons, a simple capillary tube was selected over a more complex thermostatic expansion valve, and a suction accumulator and de-superheating coils were both omitted. The result was that the final system, shown in Figure 3.2, including compressors, condenser, inter-stage heat exchanger, and receivers, could fit within a 25 cm x 40 cm x 60 cm box, for a total size of about 60000 cm³.

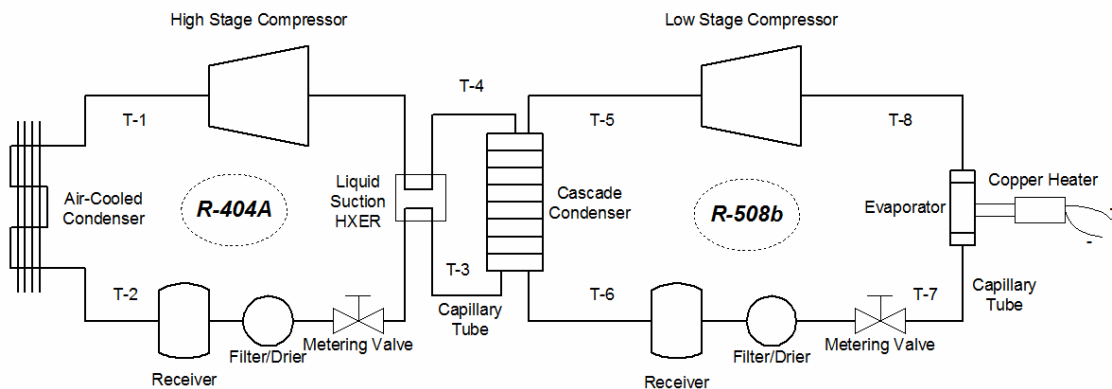


Figure 3.1: Refrigeration flow loop for a two-stage cascaded VCR system.

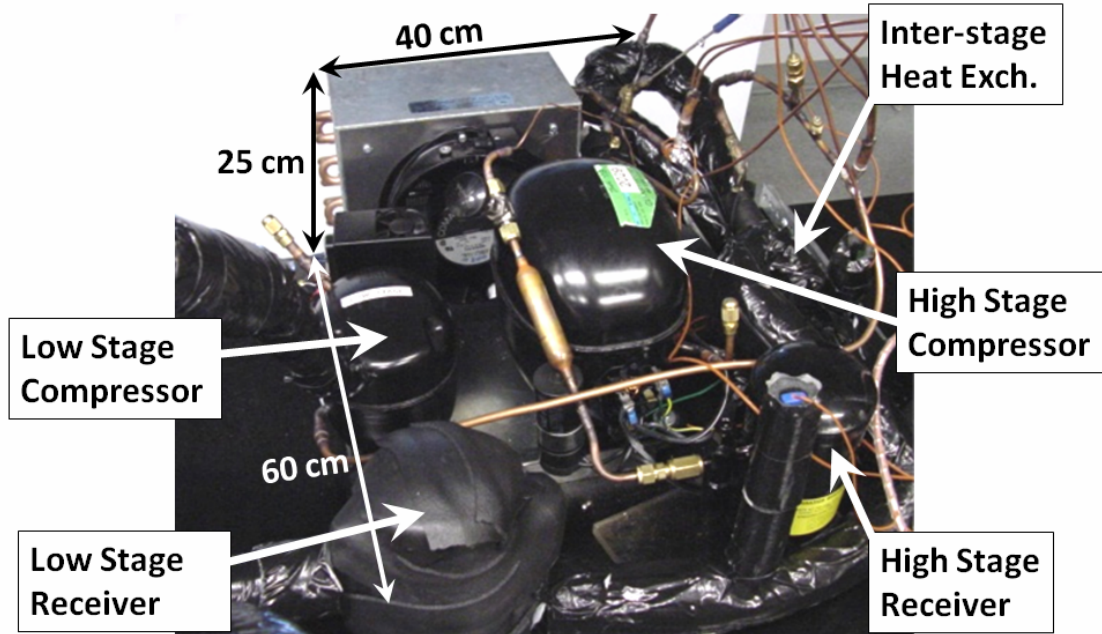


Figure 3.2: Two-stage cascaded VCR system developed in the study.

3.2.1 Compressors

The low stage compressor was selected first. Relatively few compact, powerful, inexpensive compressors are available in today's market. With a volume of $\sim 2230 \text{ cm}^3$, the Danfoss BD80F brushless DC, hermetic compressor, shown in Figure 3.3, was the smallest, most powerful, and least expensive, commercially available compressor found during this study.



Figure 3.3: Danfoss BD80F used for the low stage compressor.

This compressor is designed for R134a, and similar compressor models are sometimes used in single-stage VCR systems for electronics cooling. Because the manufacturer only provides data on this compressor for use with R134a, it is necessary to estimate the compressor's performance with R508b. By using the evaporator temperatures ($T_{evaporator}$) and cooling capacities (\dot{Q}_{in}) given in the compressor's data sheet, listed in Table 3.2, it is possible to plot the volume flow rate of the compressor versus pressure ratio. Once the volume flow rate is established, the properties of R508b are used to estimate a new mass flow rate.

Table 3.2: Performance of Danfoss BD80F operating at 4400 RPM with R134a

($T_{condenser} = 54.4$ °C; $T_{ambient} = 32$ °C; no subcooling).

$T_{evaporator}$ (°C)	-30	-25	-23.3	-20	-15	-10	-5
\dot{Q}_{in} (W)	67.6	96.1	107	130	170	218	274

The condensing temperature ($T_{condenser}$), given by the manufacturer, is used to find the compressor exit pressure (P_{high}). Because a two-phase mixture of R134a is found in the condenser, the pressure is a function of temperature only

$$P_{high} = P(T_{condenser}) \quad (3.1)$$

Similarly, the compressor inlet pressure (P_{low}) is determined using the given evaporating temperature

$$P_{low} = P(T_{evaporator}) \quad (3.2)$$

With high and low pressures known, the pressure ratio (P_r) is calculated

$$P_r = \frac{P_{high}}{P_{low}} \quad (3.3)$$

If the expansion device is assumed to be isenthalpic, the enthalpy increase (Δh) in the evaporator is estimated as the enthalpy of vaporization (h_{fg}) at P_{low} . Using the \dot{Q}_{in}

given by the manufacturer for each $T_{evaporator}$, the mass flow rate of R134a is determined for each P_r

$$\dot{m}_{R134a} = \frac{\dot{Q}_{in}}{\Delta h} \quad (3.4)$$

Using the mass flow rate and the saturated vapor volume of R134a ($v_{v,sat,R134a}$) at P_{low} , the volume flow rate is determined

$$\dot{V}_{R134a} = \dot{m}_{R134a} v_{v,sat,R134a} \quad (3.5)$$

If the volume flow rate is assumed to be the same, regardless of the refrigerant,

$$\dot{V}_{R508b} = \dot{V}_{R134a} \quad (2.6)$$

the volume of saturated vapor R508b ($v_{v,sat,R508b}$) at P_{low} can be used to estimate the mass flow rate at each given pressure ratio

$$\dot{m}_{R508b} = \frac{\dot{V}_{R508b}}{v_{v,sat,R508b}} \quad (2.7)$$

If this is done for each pair of evaporator temperature and cooling capacity, the compressor's performance with R508b can be estimated and plotted. Figure 3.4 shows that, if the BD80F operates at a pressure ratio of 5.5, it could deliver liquid R508b to the evaporator at ~0.0009 kg/s, sufficient to remove 100 W at -70 °C.

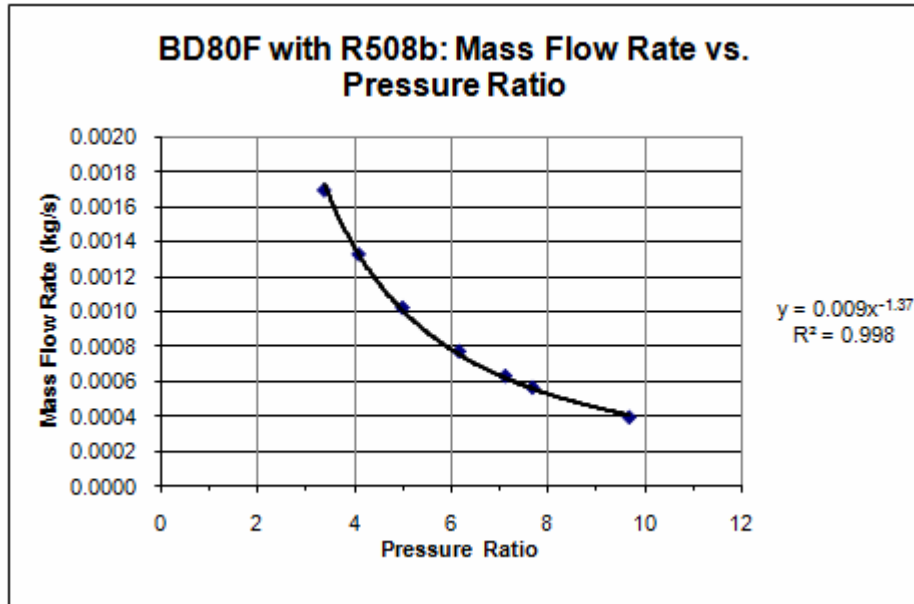


Figure 3.4: Compressor map of the Danfoss BD80F with R508b.

The same process was used to create a compressor performance map, shown in Figure 3.5, for the high stage compressor. Thus, it was determined that the 3671 cm³ Danfoss NF11FX, shown in Figure 3.6, is suitable for the high stage.

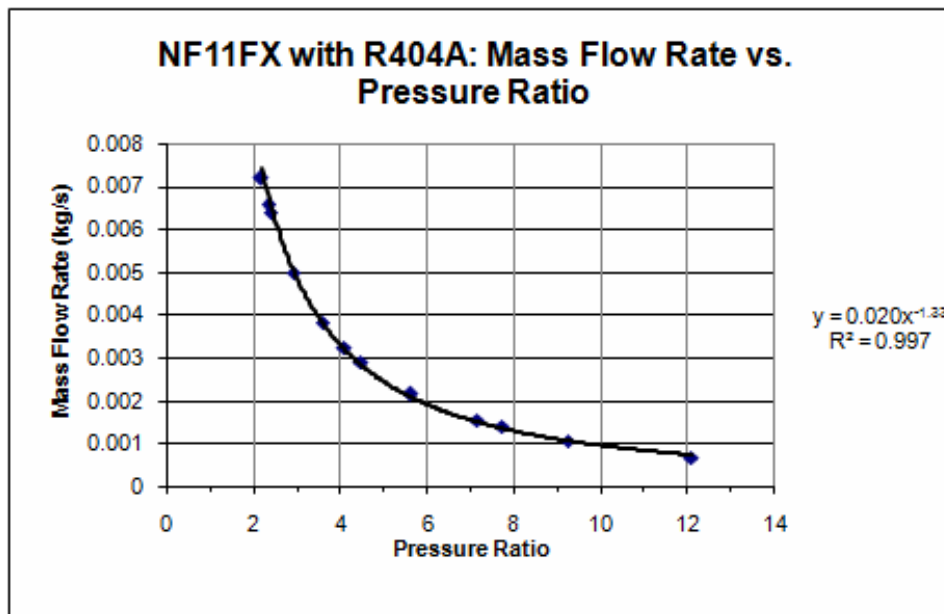


Figure 3.5: Compressor map of the Danfoss NF11FX with R404A.



Figure 3.6: Danfoss NF11FX used as high stage compressor.

3.2.2 Inter-stage Heat Exchanger

A simple concentric tube heat exchanger, originally designed as a liquid-suction heat exchanger, was used as the system's inter-stage heat exchanger. The heat exchanger, shown in Figure 3.7, was manufactured by Packless Industries (Model # HXR-50) and had a volume of 126 cm^3 . It was mounted at roughly a 45° angle. The hot vapor refrigerant from the low stage was routed through the inner tube, entering the heat exchanger from the top so that the condensing liquid would fall to the bottom. The cold liquid refrigerant from the high stage entered from bottom of the heat exchanger, so that the evaporated vapor could escape out the top.



Figure 3.7: Inter-stage heat exchanger used in the system.

3.2.3 Low Stage Evaporator

The cascade refrigeration system must interface with the microprocessor by means of a high heat flux, low temperature, compact, cold plate evaporator, appropriately insulated to avoid condensation or freezing of water on electronic components. The low stage evaporator cold plate used for this study was the alternating pin fin geometry developed in the reference [5].

3.2.4 Expansion Device

A simple capillary tube served as the expansion device in each stage. The size and length of the tubes, shown in Table 3.3, were determined using the manufacturer's recommendations, and are a function of the refrigerant properties, compressor power, and desired evaporator temperature. In order to minimize heat transfer to the expansion device while the R508b was being throttled, the low stage expansion device was placed inside of the evacuated chamber, as shown in Figure 3.8.

Table 3.3: Capillary tube information.

	Brand	Outer Diameter [cm]	Inner Diameter [cm]	Length [cm]
High Stage	Supco Bullet "Restricto"	0.18	0.07	~240
Low Stage		0.18	0.07	~300

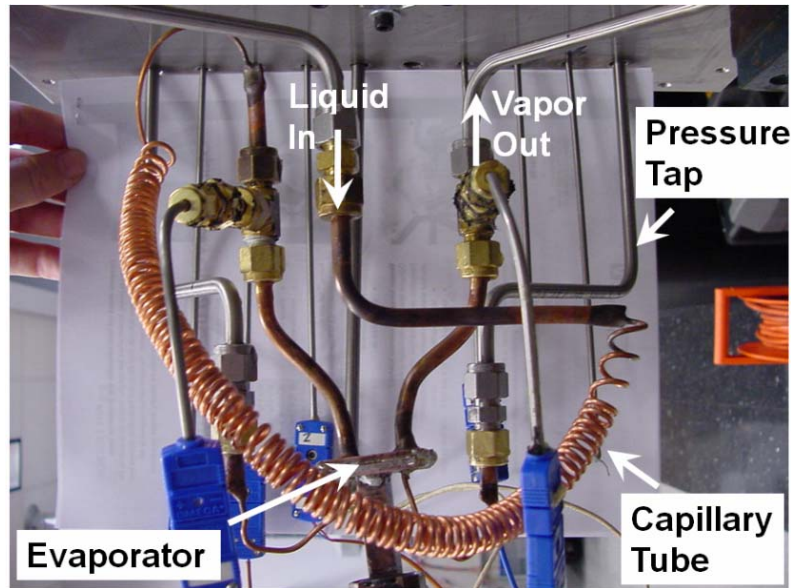


Figure 3.8: Inside the evacuated chamber housing the evaporator.

3.2.5 Air-Cooled Condenser

The air-cooled condenser, shown in Figure 3.9, was taken from a Danfoss condensing unit, and was designed for use with the NF11FX compressor used as the high stage. For safety reasons, the original fan, with unshrouded metal blades, was replaced with a COMAIR ROTRON Patriot AC (PT2B3-028254), capable of 200 CFM in low impedance conditions.



Figure 3.9: Air-cooled condenser with fan used on the high stage.

3.2.6 Miscellaneous Equipment

As shown in Figures 3.10, some additional, miscellaneous equipment was required to run the experiment and to measure and collect data. Almost all of the exposed piping was insulated with foam tubing. The exception was the copper tubing between the compressor exit and condenser inlet, which carried compressed vapor at above ambient temperatures. A power supply delivered DC power to the low stage compressor, and a control box with a variable resistor was built to control the compressor's speed. Four absolute pressure transducers and four differential pressure transducers measured the pressure at each state point. A small DC power supply and an AC transformer powered the pressure transducers. T-Type thermocouples measured temperature at each state point. An Agilent data acquisition system was used to collect the data and interface it with a personal computer using Agilent Benchlink data acquisition software.

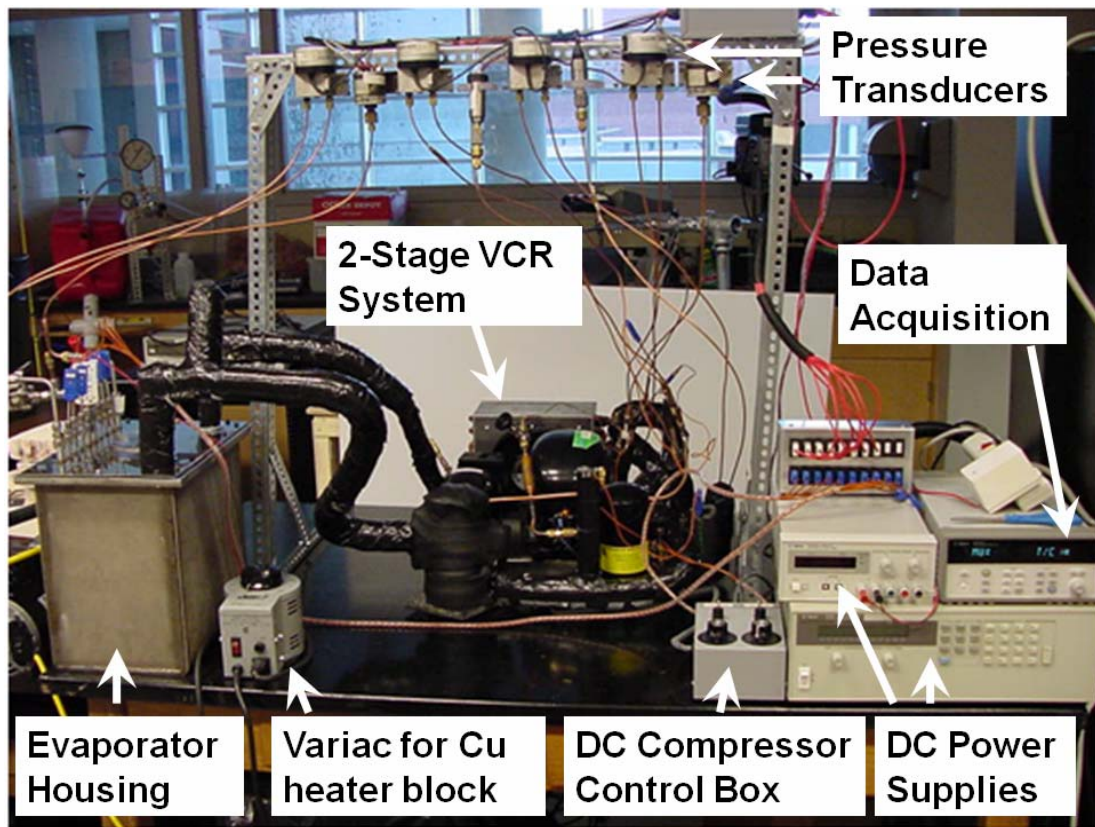


Figure 3.10: The bench-top experiment.

3.3 Test Procedure

With both compressors off, the high stage was filled with R404A until the pressures in system and the cylinder equalized. The high stage was then be started, and the compressor was allowed to draw refrigerant through the suction line port until the high stage evaporator temperature reached about $-35\text{ }^{\circ}\text{C}$. A scale was used to measure the amount of refrigerant added. With the high stage compressor on, the low stage could be prepared for operation.

The low stage compressor was charged in a similar manner. However, The BD80F was designed for R134a, and has sensing and self-diagnostic equipment that shuts the compressor off if it senses that it is operating outside of its design range (e.g., it sensed that it was too heavily loaded; it sensed that the rotor was blocked). Therefore, the low stage was much more difficult to charge and operate. Once about 0.17 kg of refrigerant was in the system, the R508b would begin to condense in the inter-stage heat exchanger. Liquid refrigerant would then begin to reach the expansion device, throttle, and cool the evaporator down to about $-80\text{ }^{\circ}\text{C}$.

With the low stage evaporator at about $-80\text{ }^{\circ}\text{C}$, a heat load could be added. By increasing the AC voltage via the variac, the heat load was increased in increments of 5 W to 10 W, and the behavior of the system was observed. The pressures and temperatures at each state point were recorded. During the experiment, the refrigerant charge in each stage could be increased or decreased, until the maximum heat load and minimum evaporator temperatures were achieved. The masses of the refrigerant charges were recorded so that experiments could be repeated with roughly the same amount of refrigerant in each stage. The heat load was increased until the system could not maintain a steady state.

3.4 Experimental Uncertainties

Temperature was measured with T-Type thermocouples with a $1.0\text{ }^{\circ}\text{C}$ limit of error. Pressure measurements had an accuracy of 0.25% Best Fit Straight Line, including linearity, hysteresis, and repeatability. The heat flux entering the evaporator

from the heater block was measured with an uncertainty of 1% [5]. The refrigerant scale had an accuracy of 0.01 kg.

CHAPTER 4

RESULTS AND DISCUSSION

4.1 Performance of the Two-Stage Cascaded VCR System

The lowest evaporator temperature recorded during the testing was $-82\text{ }^{\circ}\text{C}$ under no heat load. The highest heat load at which the system could maintain a steady state was 40 W . Under this heat load, the refrigerant was delivered to the evaporator at $-72.3\text{ }^{\circ}\text{C}$, and the chip surface temperature was maintained at $-60.5\text{ }^{\circ}\text{C}$. These conditions were achieved when the high stage was charged with 0.36 kg of R404A, and the low stage was charged with 0.24 kg of R508b. The data from this test is listed in Table 4.1.

Table 4.1: Test results of the two-stage cascaded VCR system.

Heat Input [W]	High Stage $T_{\text{evap,in}}$ [$^{\circ}\text{C}$]	High Stage $T_{\text{evap,out}}$ [$^{\circ}\text{C}$]	Low Stage $T_{\text{cond,in}}$ [$^{\circ}\text{C}$]	Low Stage $T_{\text{cond,out}}$ [$^{\circ}\text{C}$]	Low Stage $T_{\text{evap,in}}$ [$^{\circ}\text{C}$]	T_{Chip} [$^{\circ}\text{C}$]	Low Stage $P_{\text{evap,in}}$ [bar]	Low Stage $P_{\text{evap,out}}$ [bar]
0	-48.8	1.9	35.6	-15.0	-73.4	-74.5	0.986	0.786
30	-49.4	3.6	42.1	-9.8	-72.8	-65.0	1.020	0.703
40	-49.5	3.8	42.6	-9.5	-72.3	-60.5	1.076	0.703

In a later set of experiments, additional pressure transducers and thermocouples were added to the system so that all of the state points could be measured. Tables 4.2 and 4.3 list the data recorded from these experiments.

Table 4.2: Temperature measurements from the two-stage cascaded VCR system (no heat load).

Stage	Refrigerant	T_{ambient} [$^{\circ}\text{C}$]	$T_{\text{compressed}}$ [$^{\circ}\text{C}$]	$T_{\text{subcooled}}$ [$^{\circ}\text{C}$]	T_{expanded} [$^{\circ}\text{C}$]	$T_{\text{superheat}}$ [$^{\circ}\text{C}$]
High	R404A	21	47.36	21.39	-52.9	-3.52
Low	R508b	-	29.63	-22.54	-78.82	-79.59

Table 4.3: Pressure measurements from the two-stage cascaded VCR system (no heat load).

Stage	Refrigerant	$P_{\text{compressed}}$ [bar]	$P_{\text{subcooled}}$ [bar]	P_{expanded} [bar]	$P_{\text{superheat}}$ [bar]	P_r
High	R404A	12.99	12.99	2.77	2.75	4.72
Low	R508b	15.53	15.55	1.45	1.55	10.02

At a total volume of about 60000 cm³ (including compressors, air-cooled condenser, inter-stage heat exchanger, and housing), this system was about an order of magnitude smaller than the 0.4 m³ total volume of the system described by Wadell [5]. In addition to improved component matching, some of this size reduction was due to a more compact layout of the components. During this first experiment, it was determined that the high stage refrigerant receiver was unnecessary because the air-cooled condenser had enough volume to allow liquid refrigerant to collect when the system was not operating. For similar reasons, the low stage liquid receiver might also be unnecessary. Removing these bulky receivers, which were designed for much larger systems, would reduce the system size by over 2400 cm³.

4.2 Comparison of the Experimental Results and the Thermodynamic Model

The maximum heat load of 40 W was lower than the 100 W that the system was designed for. By comparing the actual performance of the system with the thermodynamic model, it was possible to diagnose the problems with the system. Figure 4.1 shows that the performance of the high stage matched closely with what the model predicted. The low stage, however, operated at a much higher P_{high} than expected. The result was a much higher pressure ratio in the low stage, and a much lower refrigerant mass flow rate.

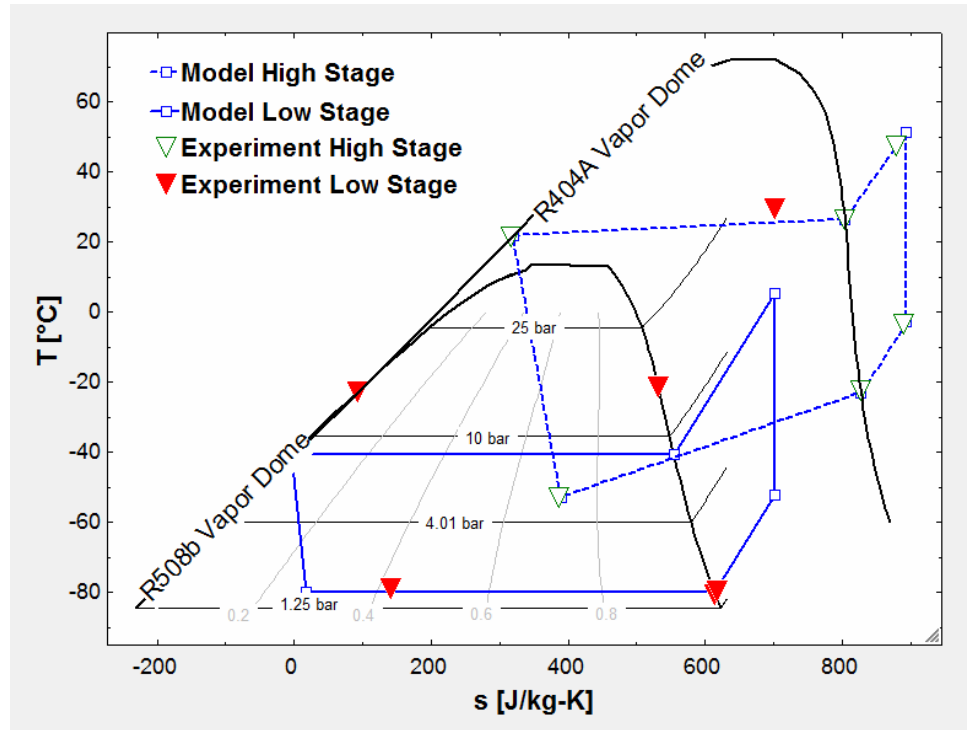


Figure 4.1: Thermodynamic Model vs. Actual Performance (no heat load).

This implies that the capacity of the low stage could be increased by increasing the effectiveness (ε) of the inter-stage heat exchanger

$$\varepsilon = \frac{\dot{Q}}{\dot{Q}_{\max}} \quad (4.1)$$

The maximum possible heat transfer rate for the exchanger (\dot{Q}_{\max}) can be described as the product of the minimum heat capacity rate (C_{\min}) and the difference of the hot and cold inlet temperatures of the heat exchanger.

$$\dot{Q}_{\max} = C_{\min} (T_{h,i} - T_{c,i}) \quad (4.2)$$

$$C_{\min} = \dot{m}c_p \quad (4.3)$$

Increasing the effectiveness of inter-stage heat exchanger would allow more heat to be removed from the low stage, and the R508b would condense at a lower condensing temperature. This would result in a lower P_{high} in the low stage. A decreased pressure

ratio across the low stage compressor would increase the mass flow rate in the low stage, which would increase the maximum capacity of the system.

In addition to improving the inter-stage heat exchanger, the system performance could be improved by minimizing heat leaks through improved application of insulation and by desuperheating the hot gas discharge from the low stage before it enters the inter-stage heat exchanger. However, these modifications would also increase the system volume.

4.3 Comparison of the Scaling Analysis and Actual VCR Systems

By adding the volumes of each component, a total system volume can be estimated. In Figures 4.2-4, the calculated volumes of the complete system, as well as the compressor and air-cooled condenser, are compared with five commercial single-stage VCR systems designed for electronics cooling, shown in Table 4.4 [7,8], and the two two-stage cascaded VCR systems developed at the Georgia Institute of Technology, shown in Table 4.5 [5,32]. The results imply that the two-stage systems are capable of increased capacity with some modifications. This reinforces an earlier conclusion that increasing the effectiveness of the inter-stage heat exchanger in the two-stage system that removed 40 W at -61 °C could increase the system capacity to ~100 W. It also appears that this system has a larger than necessary air-cooled condenser.

Table 4.4: Single-Stage VCR Systems [7,8].

	VapoChill SE	VapoChill XE	VapoChill XE II	VapoChill LS	Prometeia Mach II GT
T _{evap} [°C]	-5	-4	-18	-33	-30
Capacity [W]	130	180	180	200	200
Refrigerant	R134a	R134a	R507A	R507A	R404A
Compressor Model	Danfoss BD35F	Danfoss BD50F	Danfoss TL4CL	Danfoss FR8.4CL	Danfoss NF9FX
Compressor Volume [cm ³]	2229	2229	3767	4860	3671
Condenser Volume [cm ³]	1308	1308	2048	2250	2372

Table 4.5: Two-Stage VCR Systems [5,32].

	T _{evap} [°C]	Capacity [W]	Refrigerants (High Low)	High Stage Compressor Model (Volume [cm ³])	Low Stage Compressor Model (Volume [cm ³])	Condenser Volume [cm ³]
METTL Cascade I	-62.6	100	R134a R508b	Unknown (6000)	Unknown (6000)	3600
METTL Cascade II	-61	40	R404A R508b	NF11FX (3671)	BD50F (2229)	4032

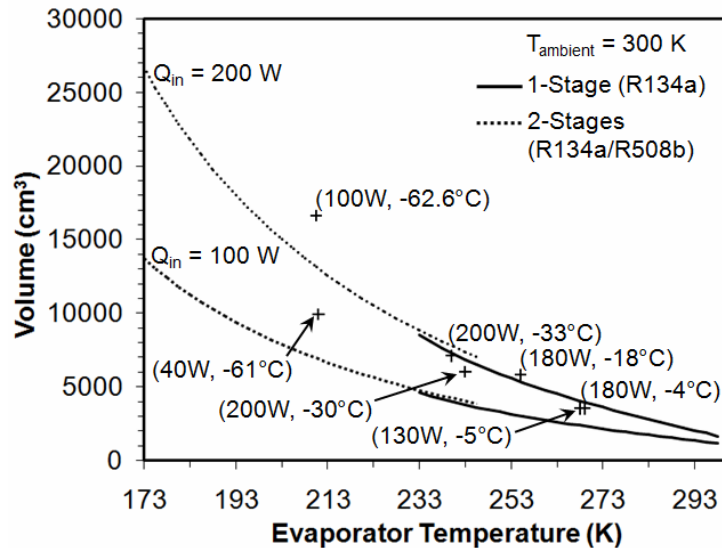


Figure 4.2: Comparing the predicted total system volume (compressor and condenser) with actual systems [5,7,8,32].

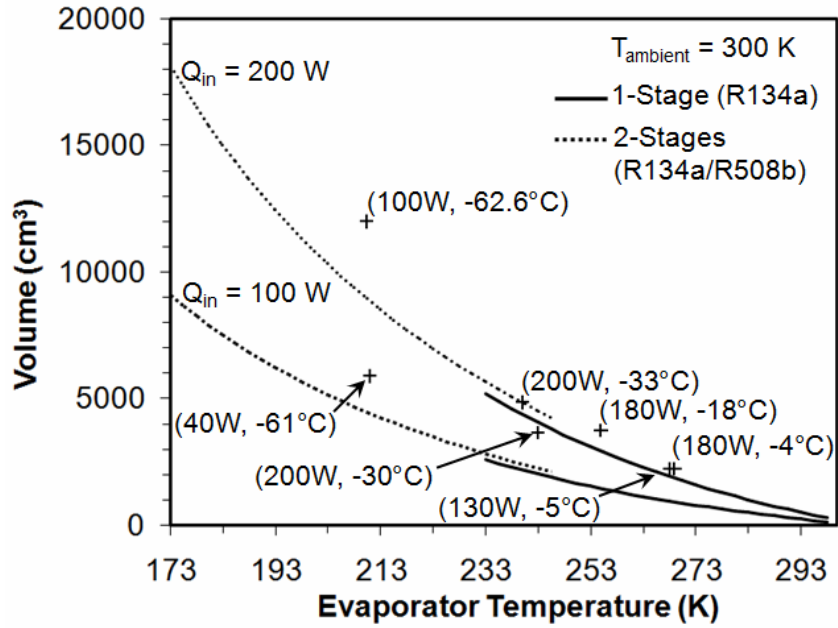


Figure 4.3: Comparing the predicted compressor volumes with compressors of actual systems [5,7,8,32].

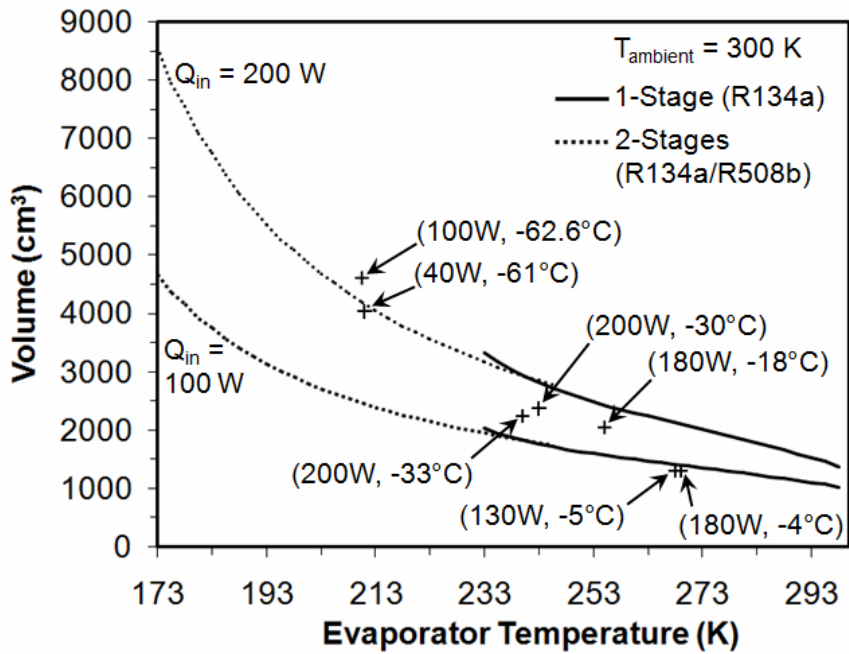


Figure 4.4: Comparing the predicted condenser volumes with condensers of actual systems [5,7,8,32].

Additional refrigerants, including R404A and R507A, were also considered in the scaling analysis. As seen in Figure 4.5, the systems using R404A and R507A are predicted to be slightly larger. With higher saturation pressures, R404A and R507A required more power to compress as compared to R134a. Therefore, the compressor will draw more power to compress these refrigerants, and they will be discharged from the compressor at higher temperatures than is R134a. A larger air-cooled condenser is required to remove the heat from the compressed vapor.

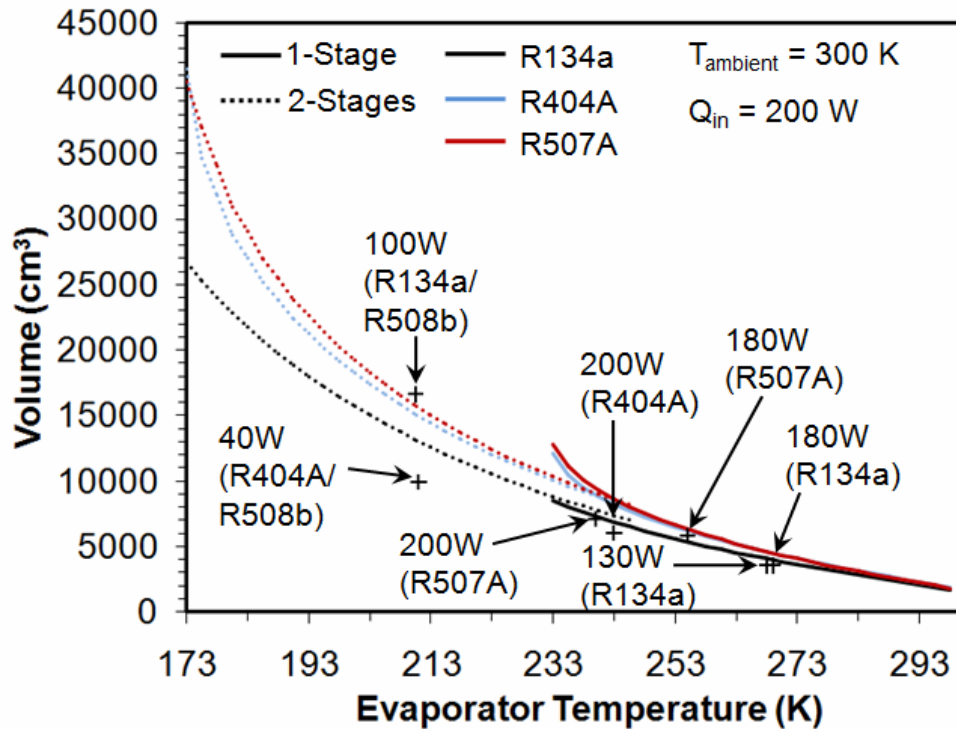


Figure 4.5: Comparing complete systems with different refrigerant combinations

[5,7,8,32].

CHAPTER 5

CLOSING

Vapor compression refrigeration offers a relatively inexpensive means of improving microprocessor performance and reliability and may be necessary in some applications to keep electronic component temperatures within recommended limits. Multiple-stage cascaded VCR systems offer the capability of evaporator temperatures lower than $-100\text{ }^{\circ}\text{C}$, and are an inexpensive alternative to cryogenic systems or open cooling cycles utilizing cryogenic fluids.

The results of the scaling analysis show that the compressor and air-cooled condenser are the largest components of any VCR system. Therefore, if the electronics industry is interested in miniaturizing sub-ambient thermal management solutions, research should focus on increasing compressor actuator power density, enhancing air-side heat transfer coefficient, and improving air-cooled condenser design. Enhancing air-side heat transfer would also benefit common heat removal components, such as heat pipes and thermosyphons. Unlike the compressor and air-cooled condenser, the problem of miniaturizing the evaporator cold plate has largely been solved.

There was moderate success in the effort to develop a small scale two-stage cascaded VCR system. At a total size of about 60000 cm^3 , the system demonstrated the capability to remove 40 Wcm^{-2} at a chip temperature of $-61\text{ }^{\circ}\text{C}$, and it is believed that the capacity could be improved to about 100 W with an improved inter-stage heat exchanger. In addition to an increased capacity, replacing the concentric tube heat exchanger with a flat plate, microchannel inter-stage heat exchanger would reduce system size further. However, in order to build a system small enough to be integrated with a desktop computer or server, smaller and more powerful compressors are still required. This is not an easy task; the attempt in this study to build a small, two-stage compression system was less than successful.

While the inter-stage heat exchanger does not occupy a significant fraction of the total system volume, its size could be reduced more easily than the compressors or the air-cooled condenser. For example, a flat plate inter-stage evaporator/condenser would be much smaller than the conventional concentric tube heat exchanger used in this study. Various analytical, computational, and experimental studies have shown that dendritic or fractal flow paths can reduce the pressure drop needed to distribute single phase fluid flow in heat exchangers [33]. In addition, prior studies have shown milled offset pin fins are effective in evaporation [5].

APPENDIX A

EES CODE FOR SCALING ANALYSIS

Engineering Equation Solver was used to perform the thermodynamic and scaling analysis. An EES Document Window provided an interface for entering input variables and system characteristics.

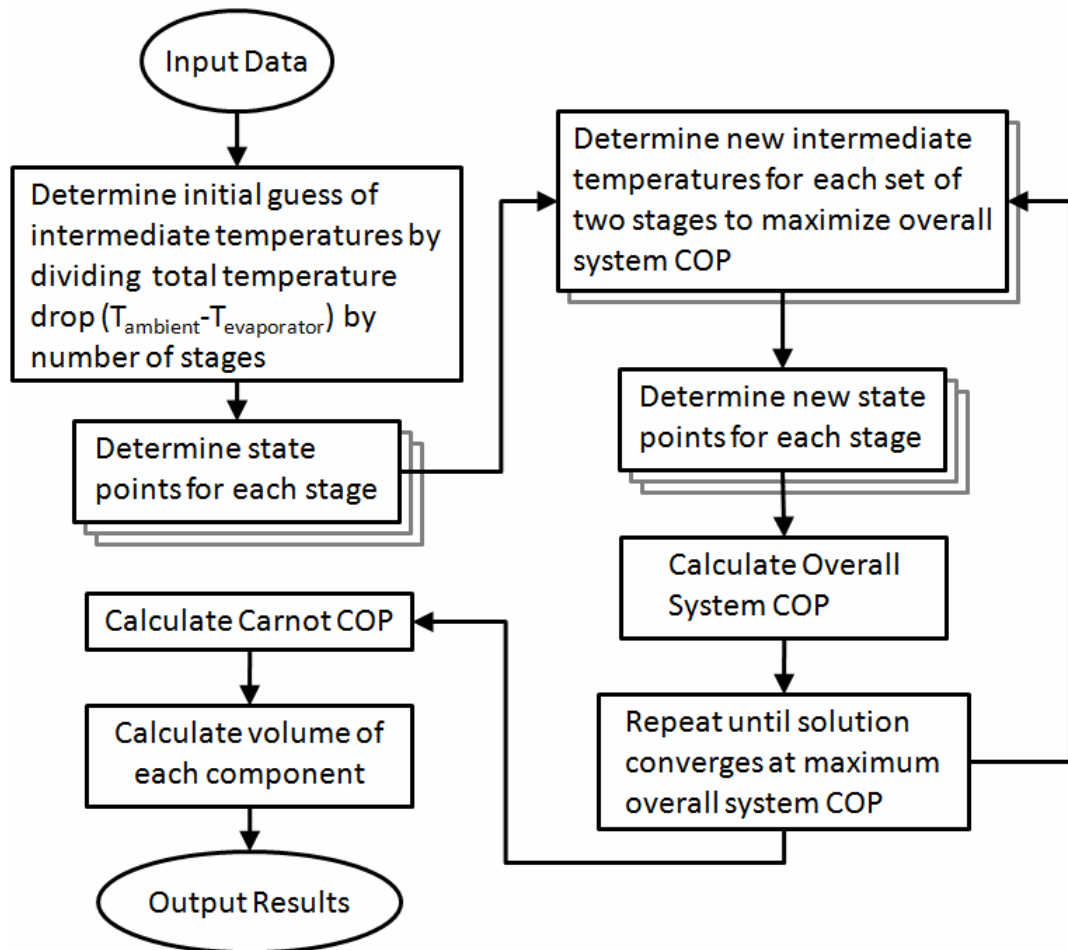


Figure A.1: Flowchart for Scaling Analysis program.

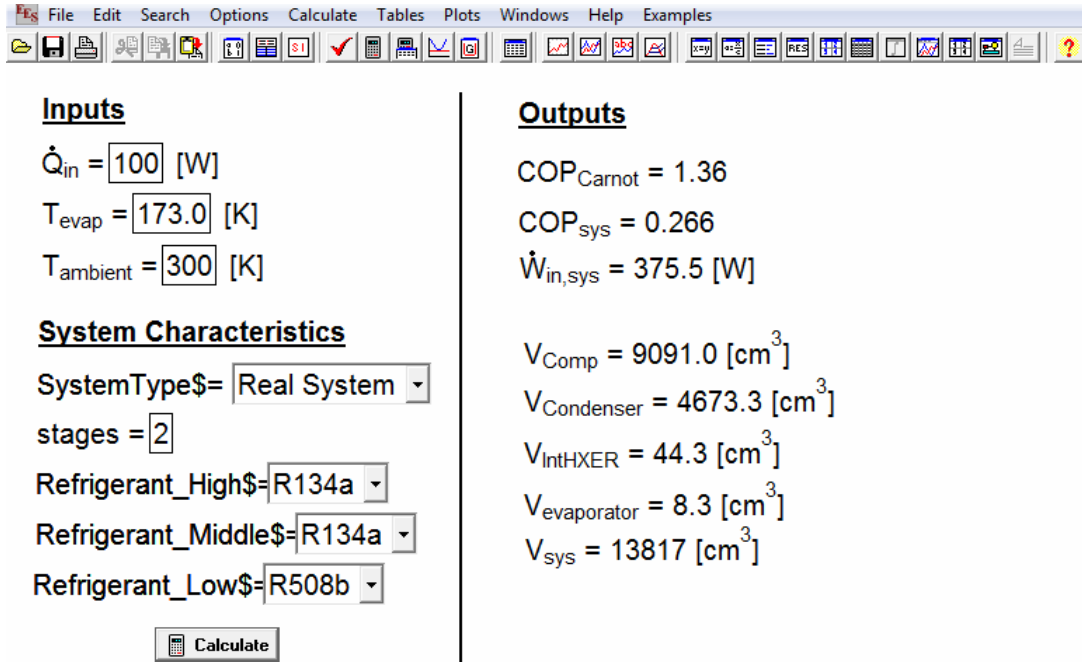


Figure A.2: EES Diagram Window for Scaling Analysis program.

Table A.1: EES Look-up Chart for j_H [27].

j_H	0.017	0.014	0.013	0.0115	0.0092	0.007	0.0058	0.005	0.0045
Re_{air}	300	500	700	900	1500	3000	5000	7000	9000

Table A.2: EES Look-up Chart for NTU [27].

NTU	0	0.5	1.0	1.5	2.0	2.5	3.0	3.5	4.0	4.5	5.0
ϵ	0	0.44	0.66	0.78	0.87	0.93	0.96	0.98	0.99	1.0	1.0

The procedures, functions, and main program were in the main body of the code, displayed below:

```

*****
"Procedure to perform the thermodynamic analysis of a single stage"
*****
PROCEDURE STAGEANALYSIS(SystemType$,T_evap,T_ambient, REF$, stage:T[1], T[2], T[3],
T[4], T[5], T[6], h[3], h[4], P_low, P_high, w_in, q_in,COP)

P_low=PRESSURE(REF$,T=T_evap,x=0.1)

```

```

IF SystemType$='Ideal System' THEN
  eta_compressor=1.0
  T_DT=0.00001 [K]
  T_AT=0 [K]
ELSE
  eta_compressor=0.4
  T_DT=5 [K]
  T_AT=2 [K]
ENDIF

```

"Choose P_high so that Condensing Temperature is slightly above T_ambient"

P_high=PRESSURE(REF\$, T=T_DT+T_ambient, x=0.5)

"1. Condensed"

```

P[1]=P_high
x[1]=0.0000001
T[1]=TEMPERATURE(REF$, P=P[1], x=x[1])
h[1]=ENTHALPY(REF$, P=P[1], x=x[1])

```

"2. Subcooled"

```

T[2]=T_ambient+T_AT
P[2]=P_high
h[2]=ENTHALPY(REF$, T=T[2], P=P[2])

```

"3. Isenthalpic Expansion"

```

P[3]=P_low
h[3]=h[2]
T[3]=T_evap
x[3]=QUALITY(REF$, h=h[3], P=P[3])

```

"4. Evaporator Out"

```

P[4]=P_low
x[4]=1
T[4]=TEMPERATURE(REF$, P=P[4], x=x[4])
s[4]=ENTROPY(REF$, P=P[4], x=x[4])
h[4]=ENTHALPY(REF$, P=P[4], x=x[4])

```

"5s. Compressor Out (isentropic compression)"

```

P_s[5]=P_high
s_s[5]=s[4]
h_s[5]=ENTHALPY(REF$, P=P_s[5], s=s_s[5])
T_s[5]=TEMPERATURE(REF$, P=P_s[5], s=s_s[5])

```

"5. Compressor Out (40% isentropic compression)"

```

P[5]=P_high
h[5]=h[4]+(h_s[5]-h[4])/eta_compressor
T[5]=TEMPERATURE(REF$, P=P[5], h=h[5])

```

"6. De-superheated"

```

P[6]=P_high
x[6]=1
T[6]=TEMPERATURE(REF$, P=P[6], x=x[6])
h[6]=ENTHALPY(REF$, T=T[6], x=x[6])

```

"Energy Analysis"

```
w_in=h[5]-h[4]
q_in=h[4]-h[3]
COP=q_in/w_in
```

```
END
```

```
*****
```

```
"Procedure to determine initial intermediate temperatures between stages and to find the optimal temperatures to maximize System COP"
```

```
*****
```

```
PROCEDURE DIVIDESTAGESANDOPTIMIZE(Q_dot_in_system,
SystemType$,stages,T_evap,T_ambient, Refrigerant_Low$, Refrigerant_Middle$,
Refrigerant_High$: stage[1..stages], REF$[1..stages], T_e[1..stages], P_Low[1..stages],
T_a[1..stages], P_High[1..stages], w_in[1..stages], q_in[1..stages],COP[1..stages],
T_1[1..stages], T_2[1..stages], T_3[1..stages], T_4[1..stages], T_5[1..stages], T_6[1..stages],
V_Compressor, V_evap, V_HXER, V_Condenser, A_fr, L_condenser, V_Motors)
```

```
"First, split stages by dividing the total temperature drop by the number of stages"
```

```
factor=0.3
T_span_stage=(T_ambient-T_evap)/stages
T_ambient[stages]=T_ambient
T_evap[stages]=T_ambient[stages]-factor*T_span_stage
T_evap[1]=T_evap
P_evap=PRESSURE('R134a', T=T_evap, x=0)
```

```
i=0
REPEAT
  REF$[i]=Refrigerant_High$
  i=i+1
UNTIL (i>3)
```

```
"Find initial set of properties"
```

```
i=stages
REPEAT
  stage[i]=i
  CALL STAGEANALYSIS(SystemType$,T_evap[i],T_ambient[i], REF$[i], stage[i]:T_1[i], T_2[i],
T_3[i], T_4[i], T_5[i], T_6[i], h_3[i], h_4[i], P_evap[i], P_high[i], w_in[i], q_in[i],COP[i])
```

```
"Outputs"
```

```
T_e[i]=T_evap[i]
P_Low[i]=P_evap[i]
T_a[i]=T_ambient[i]
```

```
"Next Stage"
```

```
i:=i-1
stage[i]=i
T_ambient[i]=T_evap[i+1]
IF (i>1) THEN T_evap[i]=T_ambient[i]-factor*T_span_stage
IF (stages=2) and (i<=1) and (P_evap<1) and (T_ambient[i]<T_crit(R508b)-5) THEN
REF$[1]=Refrigerant_Low$
IF (stages=3) and (i<=1) and (T_ambient[i]<T_crit(R508b)-5) THEN
REF$[1]=Refrigerant_Low$
UNTIL (i=0)
```

```
IF (stages=1) THEN REF$[1]=Refrigerant_High$
```

```
IF (stages=2) THEN
  REF$[1]=Refrigerant_Low$
  REF$[2]=Refrigerant_High$
```

```

ENDIF
IF (stages=3) THEN
    REF$[1]=Refrigerant_Low$
    REF$[2]=Refrigerant_Middle$
    REF$[3]=Refrigerant_High$
ENDIF

"If there are two or more stages..."
IF stages>1 THEN
    "This part of the procedure optimizes the intermediate temperature of each set of stages, and
    then the overall COP."
    N:=0
    COP_sys[n]=0
    REPEAT
        "This finds optimizes the intermediate temperature for each set of two-stages"
        n:=n+1
        i:=0
        REPEAT
            i:=i+1
            stage[i]=i
            "This finds the Two-stage COP for each intermediate temperature"
            x:=0
            COP_2Stage[x]=0
            REPEAT
                x:=x+1
                IF (x=1) THEN
                    T_intermediate[i]=T_evap[i]+0.3
                    T_ambient[i]=T_intermediate[i]
                    T_evap[i+1]=T_intermediate[i]
                ELSE
                    T_intermediate[i]=T_intermediate[i]+0.5
                    T_ambient[i]=T_intermediate[i]
                    T_evap[i+1]=T_intermediate[i]
                ENDIF
                CALL STAGEANALYSIS(SystemType$,T_evap[i],T_ambient[i], REF$[i],
            stage[i]:T_1[i], T_2[i], T_3[i], T_4[i], T_5[i], T_6[i], h_3[i], h_4[i], P_evap[i], P_high[i], w_in[i],
            q_in[i],COP[i])
                "Outputs"
                T_e[i]=T_evap[i]
                P_Low[i]=P_evap[i]
                T_a[i]=T_ambient[i]
                COP_LT=COP[i]
                CALL STAGEANALYSIS(SystemType$,T_evap[i+1],T_ambient[i+1], REF$[i+1],
            stage[i+1]:T_1[i+1], T_2[i+1], T_3[i+1], T_4[i+1], T_5[i+1], T_6[i+1], h_3[i+1], h_4[i+1],
            P_evap[i+1], P_high[i+1], w_in[i+1], q_in[i+1],COP[i+1])
                COP_HT=COP[i+1]
                "Outputs"
                T_e[i+1]=T_evap[i+1]
                P_Low[i+1]=P_evap[i+1]
                T_a[i+1]=T_ambient[i+1]
                "Find Overall COP of these two stages"
                Q_dot_LT_in=1 [J/s]
                W_dot_LT_in=Q_dot_LT_in/COP_LT
                Q_dot_LT_out=Q_dot_LT_in+W_dot_LT_in
                Q_dot_HT_in=Q_dot_LT_out
                W_dot_HT_in=Q_dot_HT_in/COP_HT

```

```

        COP_2Stage[x]=Q_dot_LT_in/(W_dot_LT_in+W_dot_HT_in)
    UNTIL (COP_2Stage[x]<=COP_2Stage[x-1])
UNTIL (i=stages-1)
"This finds the Overall System COP"
i:=0
W_dot_in_system=0 [J/s]
Q_dot_in[i]=Q_dot_in_system
W_dot_in[i]=0 [J/s]
REPEAT
    i:=i+1
    Q_dot_in[i]=Q_dot_in[i-1]+W_dot_in[i-1]
    W_dot_in[i]=Q_dot_in[i]/COP[i]
    W_dot_in_system=W_dot_in_system+W_dot_in[i]
UNTIL (i=stages)
COP_sys[n]=Q_dot_in_system/W_dot_in_system
UNTIL (ABS(COP_sys[n]-COP_sys[n-1])<=0.001)
ENDIF

"This finds the volume of each component in the system"
i:=0
V_Compressor=0 [m^3]
V_HXER=0 [m^3]
V_Motors=0 [m^3]
W_dot_in_system=0 [J/s]
Q_dot_in[i]=Q_dot_in_system
W_dot_in[i]=0 [J/s]
V_Condenser=0 [m^3]
REPEAT
    i:=i+1
    Q_dot_in[i]=Q_dot_in[i-1]+W_dot_in[i-1]
    W_dot_in[i]=Q_dot_in[i]/COP[i]
    W_dot_in_system=W_dot_in_system+W_dot_in[i]
    m_dot[i]=Q_dot_in[i]/(h_4[i]-h_3[i])
    V_Compressor=V_Compressor+COMPRESSOR(VOLUME(REF$(i), T=T_4[i], h=h_3[i]),
VOLUME(REF$(i), T=T_5[i], P=P_High[i]), m_dot[i])
    V_Motors=V_Motors+MOTOR(W_dot_in[i])
    IF (i>1) THEN V_HXER:=V_HXER+V_INTERSTAGEHXER(REF$(i-1), m_dot[i], P_high[i-1],
T_3[i], T_5[i-1], T_6[i-1], T_2[i-1])
    IF (i=stages) THEN
        CALL CONDENSER(REF$(i), T_ambient, T_5[i], T_2[i], m_dot[i], Q_dot_in_system:
A_fr, L_condenser, V_Condenser)
    ENDIF
UNTIL (i=stages)

V_evap=EVAPORATOR(Q_dot_in_system)

END
*****
"Function to find the COP of the system"
*****
FUNCTION COP_system(stages, COP[1..stages])
i:=0
COP_system=0
Q_dot_in_system=1 [J/s]
W_dot_in_system=0 [J/s]
Q_dot_in[i]=Q_dot_in_system

```

```

W_dot_in[i]=0 [J/s]
REPEAT
  i:=i+1
  Q_dot_in[i]=Q_dot_in[i-1]+W_dot_in[i-1]
  W_dot_in[i]=Q_dot_in[i]/COP[i]
  W_dot_in_system=W_dot_in_system+W_dot_in[i]
UNTIL (i=stages)

COP_system=Q_dot_in_system/W_dot_in_system

END
*****
"Compressor Volume Functions: Displacement"
*****
FUNCTION COMPRESSOR(nu_4, nu_5, m_dot)
  Speed_min=3600 [RPM]
  Speed=Speed_min*CONVERT(RPM,1/s)
  eta_volumetric=0.5
  COMPRESSOR:=m_dot*(nu_4)/Speed/eta_volumetric
END
*****
"Compressor Volume Functions: Motor"
*****
FUNCTION MOTOR(W_dot_in)
  RHO_Power=(1.7589*(W_dot_in) + 208090) "[J/s-m^3]"
  MOTOR=W_dot_in/RHO_Power
END
*****
"Air-Cooled Condenser Volume Functions: Minimum heat capacity rate"
*****
PROCEDURE C(C_ref, C_air:C_min, C_max)
  IF (C_ref<C_air) THEN
    C_min:=C_ref
    C_max:=C_air
  ELSE
    C_min:=C_air
    C_max:=C_ref
  ENDIF
END
*****
"Air-Cooled Condenser Volume Functions: j_H Look-up Chart"
*****
FUNCTION j_H(Re_air)
  j_H:=INTERPOLATE('j_H','j_H','Re_air', Re_air=Re_air) "Look-up chart is 11.20 of Incropera
and DeWitt, page 675"
END
*****
"Air-Cooled Condenser Volume Functions: NTU Look-up Chart"
*****
FUNCTION NTU(C_min, C_max, epsilon)
  C_ratio=C_min/C_max "assume C_ratio is very close to 0"
  NTU:=INTERPOLATE('NTU','NTU','epsilon', epsilon=epsilon) "Look-up chart is 11.18 of
Incropera and DeWitt, page 665"
END
*****

```

SUBPROGRAM CONDENSER(REF\$, T_air_ave, T_ref_in, T_ref_out, m_dot_ref, Q_dot_in: A_fr,
L_condenser, V_Condenser)

"This largely follows Example 11.6 of Incropera and DeWitt, Page 676"

"Fan: COMAIR ROTRON Galaxy GL48Z4 040544"

V_dot_air_e=167 [cfm] "Low Impedance"

V_fan_in=5^2*1.5

V_fan_m=V_fan_in*CONVERT(in^3, m^3)

"Air Properties"

P_air=1 [bar]

V_dot_air=V_dot_air_e*CONVERT(cfm,m^3/s)

rho_air=DENSITY('Air', T=T_air_ave, P=P_air)

m_dot_air=V_dot_air*rho_air

c_p_air=Cp('Air', T=T_air_ave)

mu_air=VISCOSITY('Air', T=T_air_ave)

Pr_air=PRANDTL('Air', T=T_air_ave)

"Refrigerant Properties"

T_ref_ave=(T_ref_in+T_ref_out)/2

mu_ref=(VISCOSITY(REF\$, T=T_ref_ave, x=0)+VISCOSITY(REF\$, T=T_ref_ave, x=1))/2

Pr_ref=(Prandtl(REF\$, T=T_ref_ave, x=0)+Prandtl(REF\$, T=T_ref_ave, x=1))/2

k_ref=(CONDUCTIVITY(REF\$, T=T_ref_ave, x=0)+CONDUCTIVITY(REF\$, T=T_ref_ave,
x=1))/2

Re_D_ref=(4*m_dot_ref)/(PI*D_i*mu_ref)

Nusselt_D_ref=0.023*Re_D_ref^(4/5)*Pr_ref^(0.4) "Page 491, Incropera and DeWitt"

h_ref=Nusselt_D_ref*k_ref/D_i

"Assume"

k_copper=k_('Copper', T_ref_ave)

k_aluminum=k_('Aluminum', T_ref_ave)

c_p_ref=Cp(REF\$, T=T_ref_ave, x=0)

"Geometry of Heat Exchanger"

D_i=0.008 [m]

D_o=0.0102 [m]

RATIO_FinArea=0.913

sigma=0.534

D_fin=0.022 [m]

alpha=587 [m^2/m^3]

A_fr=0.02 [m^2] "Frontal Area of Heat Exchanger"

D_h_flow=0.00363 [m]

t=0.00033 [m]

"Analysis of Heat Exchanger"

RATIO_Ac_Ah=D_i/D_o*(1-RATIO_FinArea)

AhRw=D_i*ln(D_o/D_i)/(2*k_copper*(RATIO_Ac_Ah)) "Area hot x Wall resistance"

G_air=m_dot_air/(sigma*A_fr)

Re_air=G_air*D_h_flow/mu_air

j_H=0.01 "j_H(Re_air)"

j_H=St*Pr_air^(2/3)

St=h_air/(G_air*C_p_air) "Stanton #"

r_2=D_fin/2

```

r_2c=r_2+t/2
r_1=D_o/2
r_RATIO=r_2c/r_1
L=r_2-r_1
L_c=L+t/2
A_p=L_c*t
FinFactor=L_c^(1.5)*(h_air/(k_aluminum*A_p))^0.5
eta_f=0.90 "From Figure 3.19"
eta_o_h=1-RATIO_FinArea*(1-eta_f)
1/U_air=1/(h_air*(RATIO_Ac_Ah))+AhRw+1/(eta_o_h*h_ref)
C_ref=m_dot_ref*c_p_ref
Q_dot_ref=C_ref*(T_ref_in-T_ref_out)
C_air=m_dot_air*c_p_air
CALL C(C_ref, C_air:C_min, C_max)
Q_dot_max=C_min*(T_ref_in-T_air_ave)
epsilon=Q_dot_ref/Q_dot_max
NTU=NTU(C_min, C_max, epsilon)
A_air=NTU*C_min/U_air
V_Condenser=A_air/alpha+V_fan_m
L_Condenser=V_Condenser/A_fr

END
*****
"Inter-stage Heat Exchanger Volume Function"
*****
FUNCTION V_INTERSTAGEHXER(REF$, m_dot, P_cond, T_evap_in, T_sh_in, T_cond_in,
T_sc_out)

"Condenser Fluid Properties"

"Geometry"
H_ch=0.000713 [m]
W_ch=0.000231 [m]
W_w=W_ch/2
W_coldplate=0.02 [m]
N_chs=W_coldplate/(2*W_ch)
A_flow=H_ch*W_ch
BETA=W_ch/H_ch
d_h=(4*H_ch*W_ch)/(2*(H_ch+W_ch))
P_ch=2*H_ch+W_ch

"Flow Conditions"
G=m_dot/(N_chs*A_flow)
q_flux_cm=93.8 [W/cm^2]
q_flux=q_flux_cm*CONVERT(W/cm^2, W/m^2)
i=0
x[0]=QUALITY(REF$, T=T_sh_in, P=P_cond)
h_f_sum=0
Q_dot[1]=0

"Desuperheated Region (gas)"
IF x[i]>1 THEN
    T_sh_ave=(T_sh_in+T_cond_in)/2
    DELTAh=ENTHALPY(REF$, T=T_sh_in, P=P_cond)-ENTHALPY(REF$, T=T_cond_in, x=1)
    DELTAT=T_sh_in-T_cond_in
    Pr=Prandtl(REF$, T=T_sh_ave, P=P_cond)

```

```

k=CONDUCTIVITY(REF$, T=T_sh_ave, P=P_cond)
mu=viscosity(REF$, T=T_sh_ave, P=P_cond)
G[i]=m_dot/(N_chs*H_ch*W_ch)
Re=d_h*G[i]/mu
Nu_D=0.023*Re^(0.8)*Pr^(1/3)
h_bar=Nu_d*k/d_h
L_sh_channel=m_dot/N_chs*DELTAh/(h_bar*DELTA*T*P_ch)
Q_dot_sh=m_dot*DELTAh
ELSE
Q_dot_sh=0 [W]
L_sh_channel=0 [m]
ENDIF
i=1

"Two-Phase Region (two-phase mixture)"
L_cond_channel=0 [m]
L_section=0.0001 [m]
x[i]=1
IF (x[i]>=0.01) THEN
h_cond_in=ENTHALPY(REF$,T=T_cond_in, x=1)
h[i]=h_cond_in
mu_cond_f=viscosity(REF$, t=T_cond_in, x=0)
rho_cond_f=viscosity(REF$, t=T_cond_in, x=0)
rho_cond_g=viscosity(REF$, t=T_cond_in, x=1)
k_cond_f=CONDUCTIVITY(REF$, t=T_cond_in, x=0)
Pr_cond_f=Prandtl(REF$, t=T_cond_in, x=0)
REPEAT
G_e[i]=G*((1-x[i])+x[i]*(rho_cond_f/rho_cond_g)^0.5)
Re_e=d_h*G_e[i]/mu_cond_f
C=5.03
n=1/3
h_f[i]=k_cond_f/d_h*C*Re_e^n*Pr_cond_f^(1/3) "Akers et al. (1959) pg 466"
h_f_sum=h_f_sum+h_f[i]
eta=1
T_w_b=T_cond_in-q_flux*(W_ch+2*W_w)/(h_f[i]*(W_ch+2*eta*H_ch))
Q_dot_section[i]=h_f[i]*N_chs*(W_ch+2*eta*H_ch)*L_section*(T_cond_in-T_w_b)
i=i+1
h[i]=h[i-1]-Q_dot_section[i-1]/m_dot
x[i]=QUALITY(REF$, T=T_cond_in, h=h_f[i])
L_cond_channel=L_cond_channel+L_section
Q_dot[i]=Q_dot[i-1]+Q_dot_section[i-1]
Q_dot_cond=Q_dot[i]
UNTIL (x[i]<=0.05)
ENDIF

"Subcooled Region (liquid)"
x[i]=0
T_sc_ave=(T_cond_in+T_sc_out)/2
DELTAh=ENTHALPY(REF$, T=T_cond_in, x=0)-ENTHALPY(REF$, T=T_sc_out, P=P_cond)
DELTA*T=T_cond_in-T_sc_out
Pr=Prandtl(REF$, T=T_sc_ave, P=P_cond)
k=CONDUCTIVITY(REF$, T=T_sc_ave, P=P_cond)
mu=viscosity(REF$, T=T_sc_ave, P=P_cond)
G=m_dot/(N_chs*H_ch*W_ch)
Re=d_h*G/mu
Nu_D=0.023*Re^(0.8)*Pr^(1/3)

```

```

h_bar=Nu_d*k/d_h
L_sc_channel=m_dot/N_chs*DELTAh/(h_bar*DELTA*T*P_ch)
Q_dot_sc=m_dot*DELTAh

```

"Exit Quality"

```
x_exit=QUALITY(REF$, T=T_sc_out, P=P_cond)
```

"Average Heat Transfer Coefficient"

```
h_f_ave=h_f_sum/i
```

"Total Heat Transfer"

```
Q_dot_condenser=Q_dot_sh+Q_dot_cond+Q_dot_sc
```

"Total Length of Inter-stage Heat Exchanger"

```
L_condenser=L_sh_channel+L_cond_channel+L_sc_channel
```

"Volume of Inter-stage Heat Exchanger"

```
V_INTERSTAGEHXER=2*(2*L_condenser)*(3*W_coldplate)*(4*H_ch)
```

END

```
*****
```

"Evaporator Coldplate Volume Function"

```
*****
```

```
FUNCTION EVAPORATOR(Q_dot)
```

```
  q_flux=93.8 [W/cm^2]
```

```
  A_evaporator=Q_dot/q_flux
```

```
  EVAPORATOR:=4*(A_evaporator^0.5+1)^2*0.5
```

END

```
*****
```

"MAIN PROGRAM"

```
*****
```

"This is the Main Program"

"INPUTS"

"note: all inputs are in EES Diagram Window"

```
{T_evap=173 [K]}
```

```
{T_ambient=300 [K]}
```

```
{Q_dot_in=100 [W]}
```

```
{SystemType$='Ideal'}
```

```
{stages=2 "Number of Stages"}
```

```
{Refrigerant_High$='R134a'}
```

```
{Refrigerant_Middle$='R404A'}
```

```
{Refrigerant_Low$='R508b'}
```

```
CALL DIVIDESTAGESANDOPTIMIZE(Q_dot_in, SystemType$, stages, T_evap, T_ambient,
Refrigerant_Low$, Refrigerant_Middle$, Refrigerant_High$: stage[1..stages], REF$[1..stages],
T_evap[1..stages], P_Low[1..stages], T_ambient[1..stages], P_High[1..stages], w_in[1..stages],
q_in[1..stages], COP[1..stages], T_Condensed[1..stages], T_Subcooled[1..stages],
T_Expanded[1..stages], T_Evaporated[1..stages], T_Compressed[1..stages],
T_Desuperheated[1..stages], V_Compressor, V_evaporator, V_HXER, V_Cond, A_fr,
L_condenser, V_Motors)
```

"System Energy Analysis"

```
COP_sys=COP_System(stages, COP[1..stages])
```

```
COP_Carnot=1/(T_ambient/T_evap-1)
```

```
Percent_Carnot=COP_sys/COP_Carnot*100
```

$$W_{\dot{\text{in}}_{\text{sys}}} = Q_{\dot{\text{in}}} / \text{COP}_{\text{sys}}$$

"Volumes of each component"

$$V_{\text{Comp}} = 5 * V_{\text{Motors}} * \text{CONVERT}(\text{m}^3, \text{cm}^3)$$

$$V_{\text{Gas}} = V_{\text{compressor}} * \text{CONVERT}(\text{m}^3, \text{cm}^3)$$

$$V_{\text{Motor}} = V_{\text{Motors}} * \text{CONVERT}(\text{m}^3, \text{cm}^3)$$

$$V_{\text{IntHXER}} = V_{\text{HXER}} * \text{CONVERT}(\text{m}^3, \text{cm}^3)$$

$$V_{\text{Condenser}} = V_{\text{Cond}} * \text{CONVERT}(\text{m}^3, \text{cm}^3)$$

"Complete System Volume"

$$V_{\text{sys}} = V_{\text{Comp}} + V_{\text{IntHXER}} + V_{\text{Condenser}} + V_{\text{evaporator}}$$

APPENDIX B

VCR SYSTEM SURVEY

Five commercial single-stage systems, and two two-stage systems were surveyed and the data was compared with the results of the scaling analysis. Only the compressor and air-cooled condenser size were considered. If the compressor model could be identified from the photo, the volume could be determined from the manufacturer's data sheets. Otherwise, the dimensions were estimated using the context in the photo. All of the air-cooled condenser volumes were estimated by estimating the dimensions from the photographs. The volume of the fan was included in the total volume of the air-cooled condenser.

VapoChill SE

Rated Capacity and Evaporator Temperature: 130 W @ -5 °C

Refrigerant: R134a

Compressor (Volume): Danfoss BD35F (2229.3 cm³)

Volume of Air-Cooled Condenser, including fan: 1307.6 cm³



Figure B.1: The VapoChill SE [7]

VapoChill XE

Rated Capacity and Evaporator Temperature: 180 W @ -4 °C

Refrigerant: R134a

Compressor (Volume): Danfoss BD50F (2229.3 cm³)

Volume of Air-Cooled Condenser, including fan: 1307.6 cm³



Figure B.2: The VapoChill XE [7].

VapoChill XE II

Rated Capacity and Evaporator Temperature: 180 W @ -18 °C

Refrigerant: R507A

Compressor (Volume): Danfoss TL4CL (3766.7 cm³)

Volume of Air-Cooled Condenser, including fan: 2048.0 cm³



Figure B.3: The VapoChill XE II [7].

VapoChill LightSpeed

Rated Capacity and Evaporator Temperature: 200 W @ -33 °C

Refrigerant: R507A

Compressor (Volume): Danfoss FR8.4CL (4860.4 cm³)

Volume of Air-Cooled Condenser, including fan: 2250.0 cm³



Figure B.4: The VapoChill Light Speed [7].

Prometeia Mach II GT

Rated Capacity and Evaporator Temperature: 200 W @ -30 °C

Refrigerant: R404A

Compressor (Volume): Danfoss NF9FX (3671.3 cm³)

Volume of Air-Cooled Condenser, including fan: 2371.6 cm³



Figure B.5: The Prometeia Mach II GT [8].

Two-stage cascaded VCR system developed in [5]

Rated Capacity and Evaporator Temperature: 100 W @ -62.6 °C

High Stage Refrigerant: R134a

High Stage Compressor (Volume): Unknown (6000 cm³)

Low Stage Refrigerant: R508b

Low Stage Compressor (Volume): Unknown (6000 cm³)

Volume of Air-Cooled Condenser, including fan: 3600 cm³



Figure B.6: The two-stage cascaded VCR system used to test compact evaporators [5].

Two-stage cascaded VCR system developed in current study

Rated Capacity and Evaporator Temperature: 40 W @ -61 °C

High Stage Refrigerant: R404A

High Stage Compressor (Volume): Danfoss NF11FX (3671.3 cm³)

Low Stage Refrigerant: R508b

Low Stage Compressor (Volume): Danfoss BD80F (2229.3 cm³)

Volume of Air-Cooled Condenser, including fan: 4032 cm³

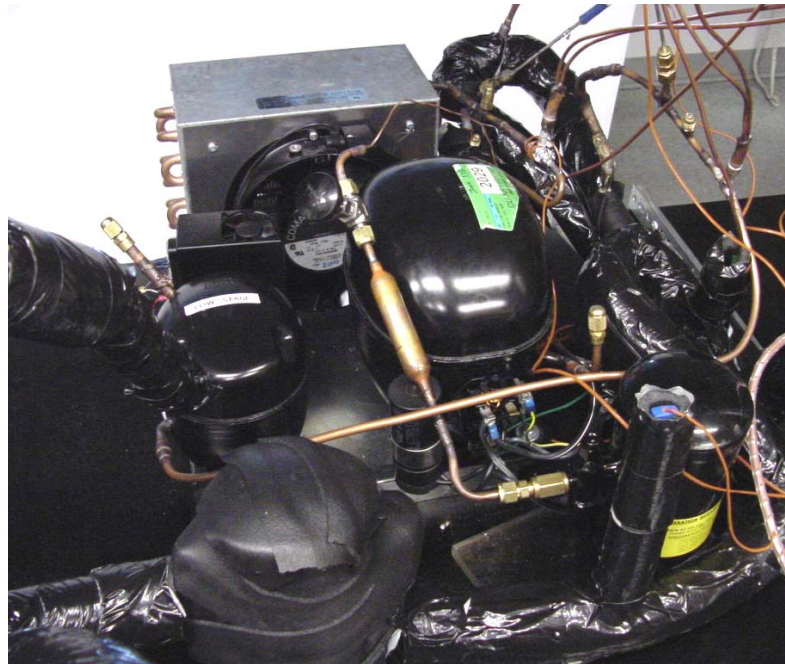


Figure B.7: The two-stage cascaded VCR system developed in this study.

APPENDIX C

DESIGN OF A TWO-STAGE CASCADED VCR SYSTEM USING A MODIFIED AIR COMPRESSOR

C.1 System Design Concept

A two-stage VCR system would still need to be about 1/7 smaller than the system described in Chapter 3 before it could be integrated with a high performance desktop. Therefore, a second experimental system was designed in an attempt to further reduce the system volume. The compressors, as the largest components of the system, provided the greatest opportunity for size reduction. Several ideas were considered to reduce the size of the compression system. A compact, diaphragm membrane compressor was considered, similar to the concepts under development [34,35]. However, none of these compressors were successfully fabricated, and it was doubtful that such a compressor could even deliver the high pressure ratios required in this cycle. Small scale, scroll compressors from the company Air Squared were considered, but the company concluded their product was not appropriate for this application. It was also attempted to acquire small and powerful rotary compressors from the Tecumseh Products Company, but their product was still under development and would not be available for this project.

The next consideration was to modify off-the-shelf reciprocating compressors, similar to the ones used in the first experiment, which were demonstrated to be capable of the high pressure ratios and flow rates required for the system. Several compressors, including the one shown in Figure C.1, were dismantled to identify the major components and their corresponding volumes.

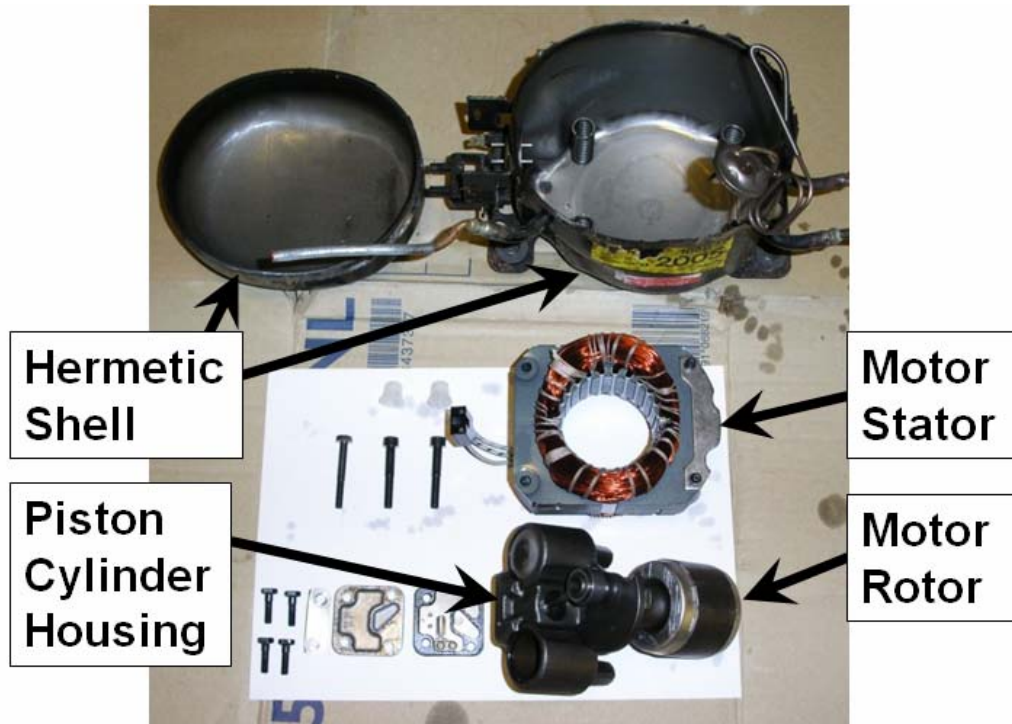


Figure C.1: A small, hermetic compressor, dismantled.

The motor is by far the largest component inside the compressor. The piston cylinder is in a cast iron housing bolted to the motor, and the hermetic shell enclosing all of the compressor's components is about 5 times larger than the motor. Viewing the dismantled compressor reinforced the assumption that these compressors were designed for power efficiency, ease of manufacture, low initial cost, and durability.

A recent study [20] demonstrated that an inexpensive air compressor could be modified to operate as a refrigeration compressor in a personal cooling suit for use in extreme environments. The total system developed in this study was light weight and compact enough to be worn on one's back. The compressor, using R134a and actuated by a small scale combustion engine, was powerful enough to remove 300 W at an evaporator temperature of 28 °C and an ambient temperature of 43.3 °C. This concept showed the most promise for achieving the drastic system volume reduction required for this study.

While considering the layout of a two-stage VCR system utilizing modified air compressors, it was thought that system could be built more compactly if one motor was

used instead of two. Figure C.2 shows the initial concept of the system, and C.3 shows the system schematic. The system is simplified by removing the liquid-suction heat exchanger, refrigerant receivers, and metering valves.

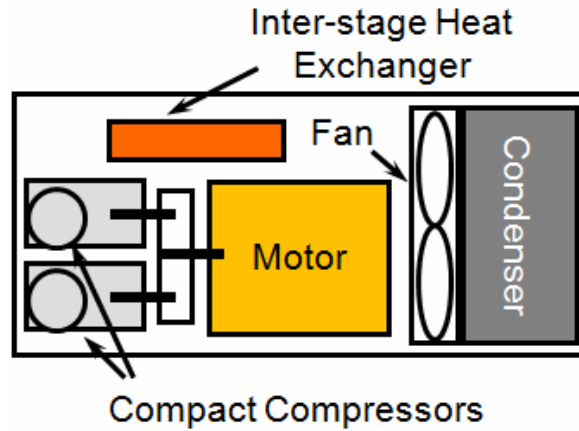


Figure C.2: Proposed layout for a two-stage cascaded VCR system using one motor.

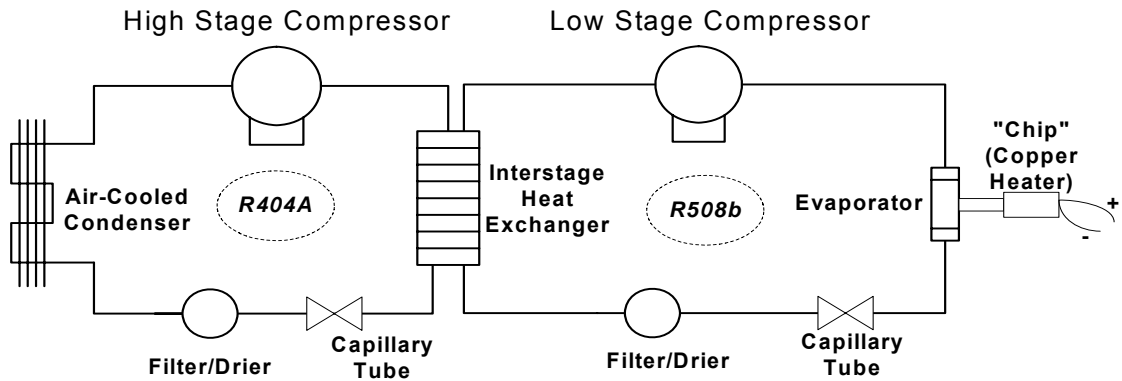


Figure C.3: Schematic of the proposed two-stage cascaded VCR.

C.2 Compressor Design and Fabrication

The compressor design and fabrication was similar to work described in reference [20]. However, there were some important differences, most noticeably that the current system would require a second compressor, and that both compressors would be driven by a single motor, instead of a small-scale combustion engine. Two inexpensive tire inflators (\$20-40), shown in Figure C.4, were purchased. Although the compressors were sold under different brands, both used identical air compressors,

shown in Figure C.5. These were, in fact, identical to the compressor that was used in [20]. All are manufactured by COIDO Corporation in Shanghai, China. The compressors are rated for pressures of at least 250 psig (17.2 bar), so it was feasible that they could operate at high pressures required in cycle using R508b.

A high torque, high speed permanent magnet DC motor, shown in Figure C.6, was selected (surplus "Triple Play Motor" from Herbach and Rademan). Table C.1 shows the motor's performance with an input of 48 VDC, a little over half of the motor's maximum rated input of 90 VDC.



Figure C.4: Two inexpensive, commercially available, tire inflators.



Figure C.5: Small air compressor manufactured by the COIDO Corporation [20].



Figure C.6: Permanent magnet DC motor selected to drive the compressor.

Table C.1: Motor performance chart.

Lab Test at 48 VDC (maximum rated voltage is 90 VDC)			
Speed (RPM)	Load (in.-lb.)	Load (Nm)	Current (amps)
3500	0	0	0.94
3000	3	0.34	2.8
2500	6	0.68	5.1
2000	9	1.02	7.4
1400	12	1.36	9.8

In Table C.2, an initial comparison of the compressors used in Chapter 3 with the modified air compressors and motor showed that a 1/5 volume reduction and a 1/4 mass reduction could be gained. Such a volume reduction in the compression system would allow the system to fit within the target dimensions. Calculations that considered the displacement and estimated operating speed of the modified air compressors showed that the new system could achieve almost 2/3 of the potential performance of the system described in Chapter 3, or a little over 60 W at -62 °C.

Table C.2: Comparison of new design and first experimental system.

High Stage Compressor			
	NF11FX	Modified Air Compressor	Change
Displacement (cm ³)	11.14	4.92	44%
Rotational Speed (RPM)	3450	3000	87%
Nominal Flow Rate (cm ³ /s)	640.55	246	38%
Size (cm ³)	3671	350	10%
Mass (kg)	9.98	0.73	7%

Low Stage Compressor			
	BD80F	Modified Air Compressor	Change
Displacement (cm ³)	3	4.92	164%
Rotational Speed (RPM)	4000	1500	38%
Nominal Flow Rate (cm ³ /s)	200	123	62% of Performance
Size (cm ³)	2229	350	16%
Mass (kg)	4.40	0.73	17%

Motor			
	N/A	Triple Play Motor	
Max Rot. Speed (RPM)	N/A	6000	
Size (cm ³)	N/A	552.9	
Mass (kg)	N/A	2.41	

	First Experimental System	Second Experimental System	Change
Total Size (cm³)	5900	1253	1/5 of Volume
Total Mass (kg)	14.4	3.9	1/4 of Mass

This volume reduction and estimated performance was encouraging, and work proceeded to fabricate a transmission hub, intake manifold, and crank case cap. These components, shown with the compressor in Figure C.7, were required to seal the compressor so that it could use refrigerant instead of air. A 1/4" copper tube that connected the intake manifold to the crankcase cap equalized the pressure on both sides of the piston and provided backside pressure that smoothed operation. Without this pressure equalization, the starting torque would be too high for the crankshaft to be rotated.

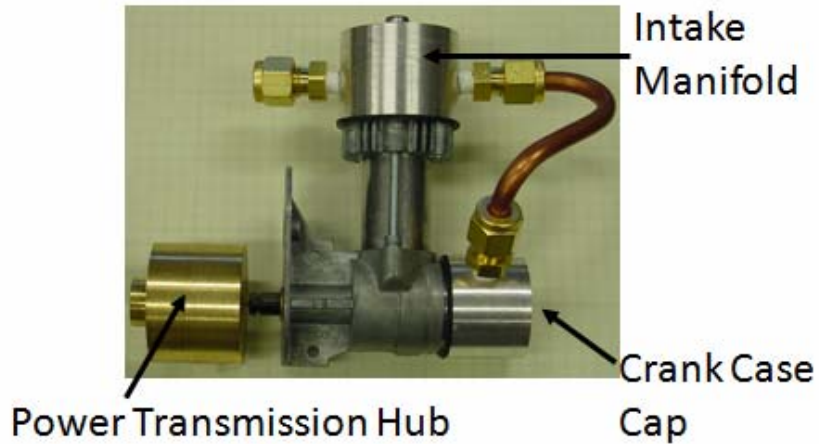


Figure C.7: Air compressor with additional components required to convert it into a compressor suitable for refrigerants.

To transmit power from the motor to the compressor, a slotted disc coupling connected the 1/4" diameter miniature precision steel drive shaft to the compressor crankshaft. The coupling was attached to the drive shaft, shown in Figure C.8, with two set screws, offset 90 degrees. Two bronze plain sleeve bearings, compression fit to the shaft, minimized the shaft's axial movement and reduced wear. While some leakage in a semi-hermetic compressor is inevitable, three spring loaded, PTFE rotating seals (1/4" inner diameter, 3/8" outer diameter, 1/16" wide) around the drive shaft minimized leakage of the refrigerant through the power transmission hub.

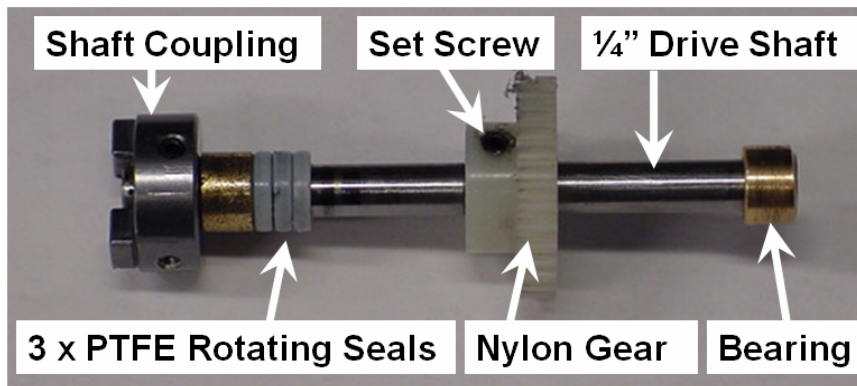


Figure C.8: Crank shaft with flexible coupling, bearings, rotating seals, and gear.

A gear train would decrease the rotational speed transferred to the drive shaft, and increase the torque. The design of the gear train depended on the motor torque/speed curve, the compressor performance, and gear availability. An initial estimate put the operating speed of the low stage at half the speed of the high stage, and the high stage operating speed at half that of the motor. In other words, the gear ratio would be 4:2:1 for low:high:motor. In order to determine if this design would be appropriate, it was necessary to estimate the maximum and average torques required to compress R404A and R508b. This was done by determining the force-time function within the compressor's cylinder, and the torque-time function acting on the input shaft of the compressor during any one cycle. The method used is described in [36], and Figures C.9 and C.10 show the resulting torque from the gas force (T_g), inertial force (T_i), and the sum of the two, or total torque (T). For R404A, the maximum torque is 9 lbf-in (1.02 Nm), and it is 13.3 lbf-in (1.50 Nm) for R508b. This means that if there is a, the motor would need to deliver a torque of 4.5 lbf-in (0.51 Nm). Likewise, if there was a 2:1 gear ratio from the low stage to the motor, the motor would need to provide a torque of 3.3 lbf-in (0.38 Nm).

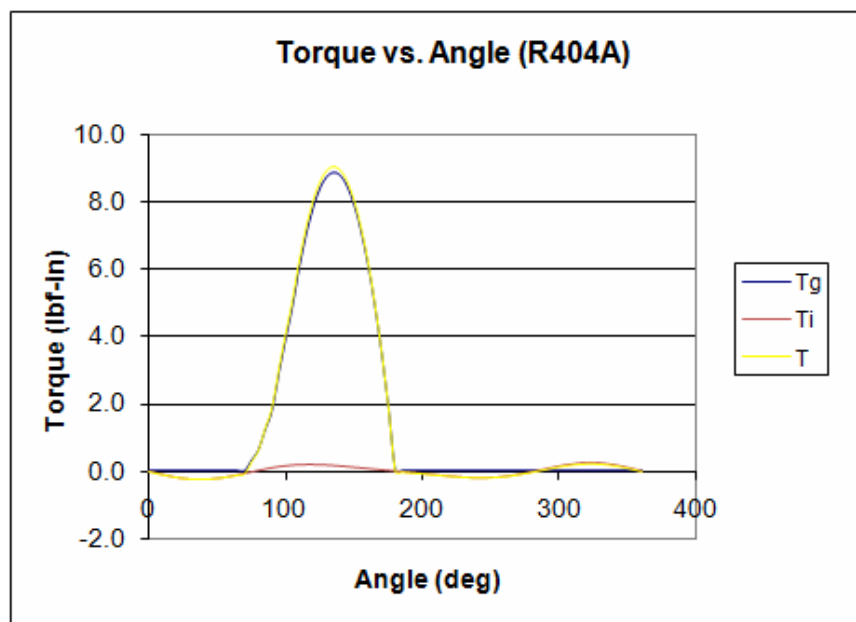


Figure C.9: Torque vs. Angle curve for compressor operating with R404A.

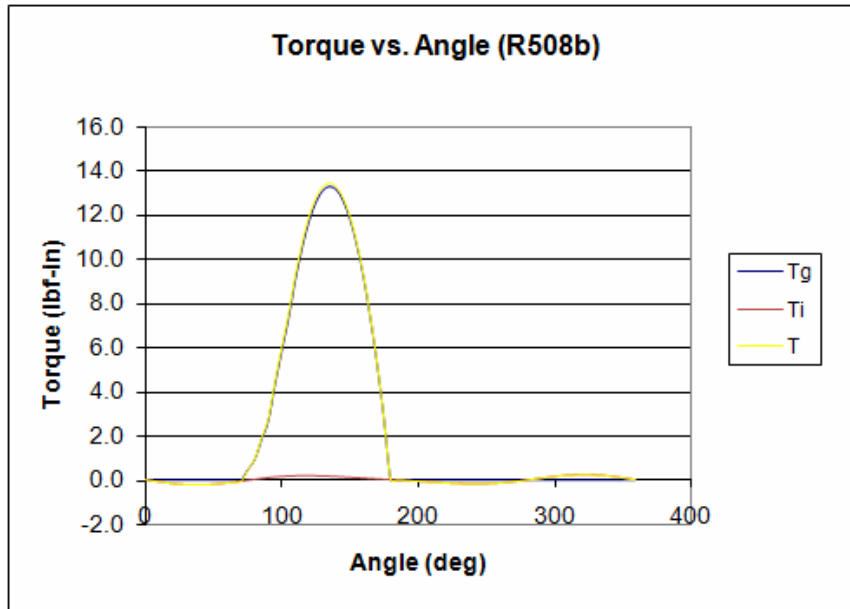


Figure C.10: Torque vs. Angle curve for compressor operating with R508b.

Using the manufacturer's data, a speed-torque curve was developed for the motor. The motor's performance at inputs of 75 VDC and 90 VDC was estimated. As shown in Figure C.11, if the maximum load is 7.8 lbf-in and the motor is operating at full power, the motor speed will be ~4800 RPM. Therefore, at a 2:1 gear ratio, the high stage will rotate at ~2400 RPM. Similarly, at a 4:1 gear ratio, the low stage will rotate at ~1200 RPM.

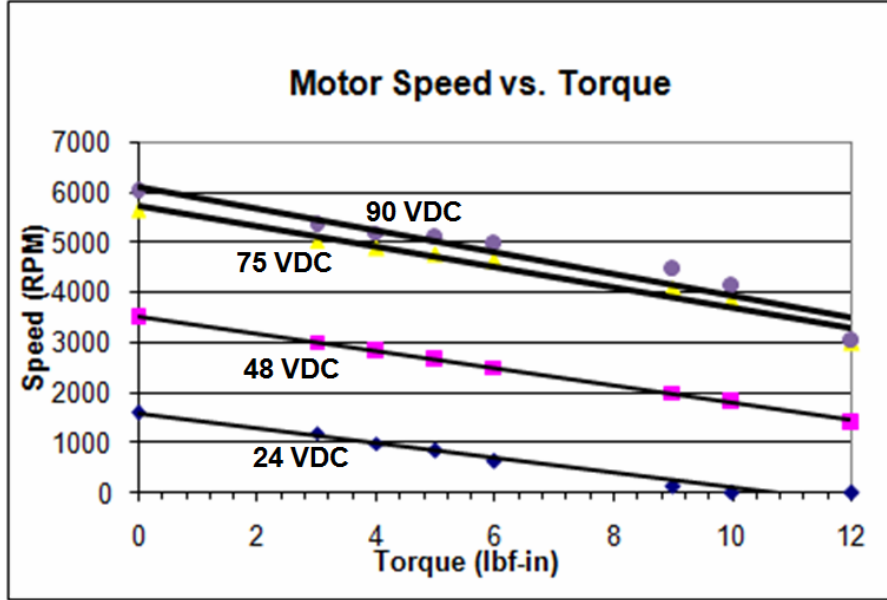


Figure C.11: Plot of motor speed versus motor torque.

The mass flow rate of each compressor was estimated using a method developed for representing compressor calorimeter test data [37]. The mass flow rate of the compressor ($\dot{m}_{compressor}$) can be estimated as a function the displacement ($V_{displacement}$), frequency (RPM), refrigerant suction volume ($v_{suction}$), and volumetric efficiency (η_v)

$$\dot{m}_{compressor} = \eta_v \frac{V_{displacement} \cdot RPM}{60v_{suction}} \quad (C.1)$$

The compressor's volumetric efficiency is estimated as

$$\eta_v = 1 - C \left[\left(\frac{P_{discharge}}{P_{suction}} \right)^{\frac{1}{k}} - 1 \right] \quad (C.2)$$

where C is the effective clearance volume ratio, estimated to be 0.1, $P_{discharge}$ is the absolute discharge pressure, $P_{suction}$ is the absolute suction pressure, and $1/k$ is the polytropic compression exponent, where

$$k = \frac{c_p}{c_v} \quad (C.3)$$

The resulting plots of mass flow versus pressure ratio for the compressor using R508b at 1200 RPM and R404A at 2400 RPM are shown in Figures C.12 and C.13.

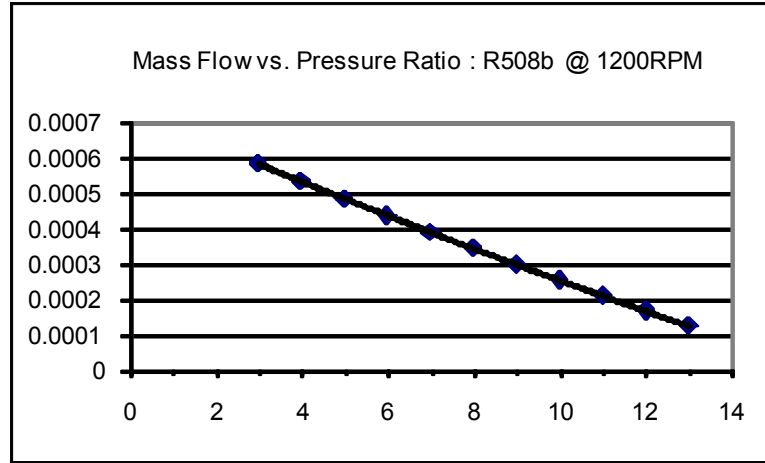


Figure C.12: Predicted performance for the compressor using R508b.

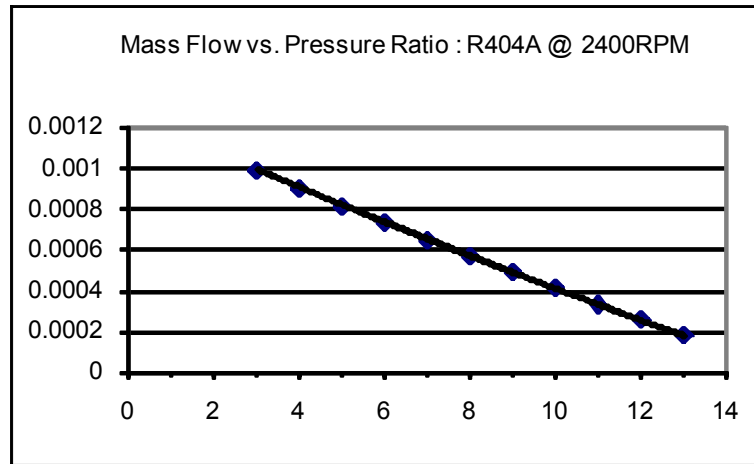


Figure C.13: Predicted performance for the compressor using R404A.

To estimate the performance of the system, these mass flow curves were input into the thermodynamic rate model. The resulting performance estimate is that a two-stage system using the modified air compressors could remove between 50 W and 75 W at an evaporator temperature of -70 °C. With an appropriately sized inter-stage heat exchanger, the high stage operating at twice the speed of the low stage should provide a sufficient mass flow rate to remove all of the heat generated and transported by the low

stage. It was conceivable that the system cooling capacity could be increased by transferring more power from the high stage to the low stage. However, because of the many assumptions already included in the analysis, the more conservative gear ratio of 4:2:1 was kept. After several design iterations, the gear train shown in Figure C.14 was developed. While inexpensive nylon gears were used in early iterations, steel gears were necessary in the final design to withstand the high torque and friction.

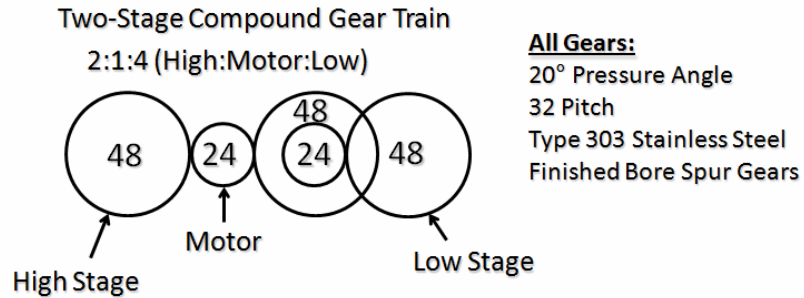


Figure C.14: Gear train design.

C.3 Changes in Refrigeration Flow Loop

While the intent was to build two compressors and test them in a cascade cycle, only a single compressor, shown in Figure C.15, was actually tested. This was because measurements from a newly added mass flow meter showed that the system would have an insufficient mass flow rate to remove even 60 W at -70 °C. The liquid-suction heat exchanger, receiver, and adjustable valve from the previous experiment were all deemed unnecessary, and thus were also removed from the flow loop. Otherwise, the bench-top experiment, shown in Figure C.16, remained relatively similar to the previous experiment.

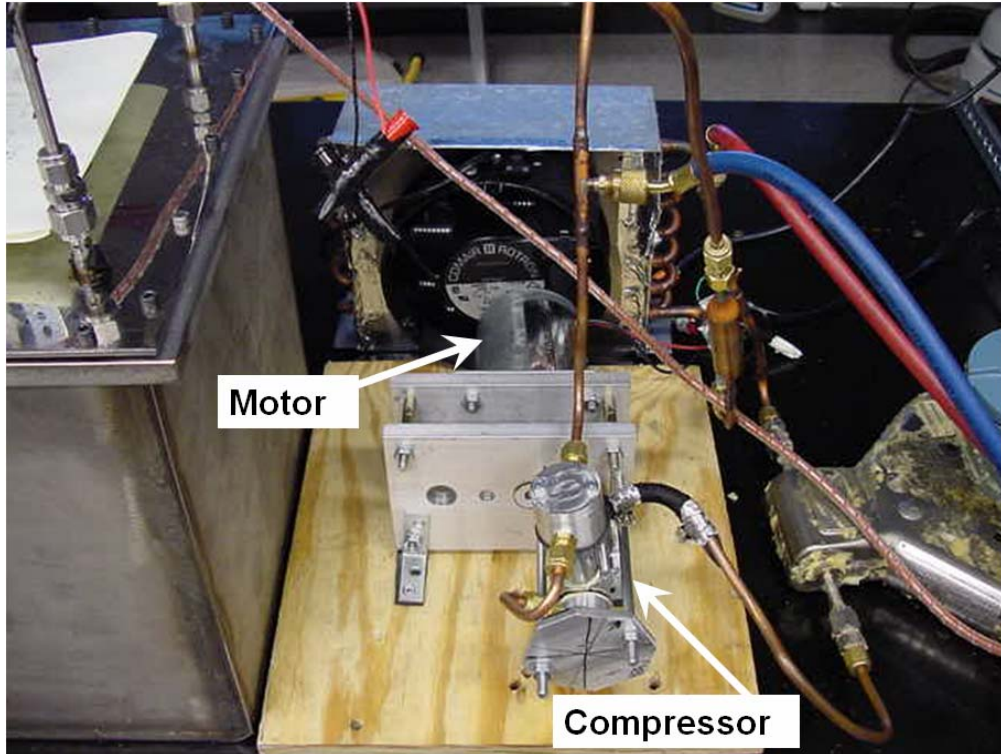


Figure C.15: Compressor, Condenser, Evaporator Housing, and mass flow meter.

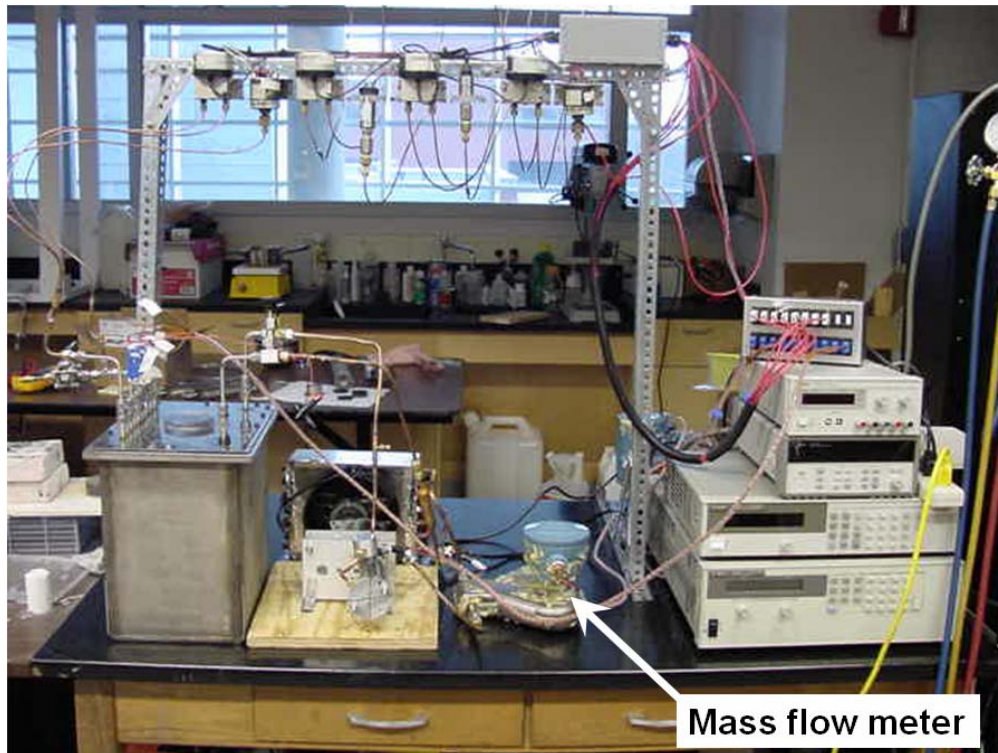


Figure C.16: The bench-top experiment for testing the compressor.

C.4 Test Procedure

System testing began with the relatively low pressure R134a, and the system was prepared for testing in the same manner as was the system described in Chapter 3. The voltage supplied to the motor was controlled by a DC power supply. The voltage could be increased to increase the speed of the compressor (at ~30 VDC, the compressor would operate at ~1000 RPM). The suction port valve was opened, and refrigerant was drawn into the system until the refrigerant reached saturation pressure in the condenser, and liquid refrigerant was throttled in the expansion device. A data acquisition system recorded the evaporator and chip temperatures, system high and low pressures, and the mass flow rate.

C.5 Experimental Uncertainties

The uncertainties associated with the temperature, pressure, and heat flux measurements remained unchanged from those described in Chapter 3. The uncertainties associated with the mass flow rate measurements were estimated to be less than $2 \times 10^{-6} \text{ kgs}^{-1}$.

C.6 Performance of Compressor

After several iterations of the design process, a single compressor was able to compress R134a and achieve no-load evaporator temperatures of $-22 \text{ }^\circ\text{C}$, sustained at about $-20 \text{ }^\circ\text{C}$. However, when mass flow measurements were taken, it was determined that at best, a two-stage system could only remove 10 W to 20 W at an evaporator temperature of $-70 \text{ }^\circ\text{C}$. When the motor power and compressor speed were increased, the mass flow rate could not be maintained above $0.000233 \text{ kgs}^{-1}$. Therefore, it was suspected that the compressor speed was exceeding the maximum rate at which the simple reed valves could actuate, thus limiting the maximum mass flow of the compressor.

REFERENCES

- [1] Semi-conductor Industry Association, *International Technology Roadmap for Semiconductors*, 2006 Update.
- [2] Phelan P., Chiriac V., Lee T.T., "Current and Future Miniature Refrigeration Cooling Technologies for High Power Microelectronics," *Proceedings of the Seventeenth SEMI-THERM Symposium*, IEEE, 2001, p. 158-167.
- [3] Naeemi A., Meindl J.D., "An upper limit for aggregate I/O interconnect bandwidth of GSI chips constrained by power dissipation," *Proceedings of the International Interconnect Technology Conference*, IEEE, 2004, p. 157-159.
- [4] Schmidt R.R., Notohardjono B.D., "High-end Server Low-Temperature Cooling," *IBM Journal of Research and Development* 46, no. 6 (2002): 739-751.
- [5] Wadell R., *Experimental Investigation of Compact Evaporators for Ultra Low Temperature Refrigeration of Microprocessors*, M.S. Thesis, Georgia Institute of Technology, 2005.
- [6] Peeples J., "Vapor Compression Cooling for High Performance Applications," *Electronics Cooling* 7, no. 3 (2001).
- [7] Asetek, Inc., www.asetek.com. Accessed March 2007.
- [8] Sun C., "Prometeia Mach II GT Phase Change Cooler Review," <http://www.pcstats.com/articleview.cfm?articleID=1793>, 2005. Accessed March 2007.
- [9] jinu117, "Xtreme Phase Gallery," <http://www.xtremesystems.org/forums/showthread.php?t=54663>, 2006. Accessed March 2007.
- [10] Ellsworth M.J., Schmidt R.R., Angonafer D., "Design and Analysis of a scheme to mitigate condensation on an assembly used to cool a processor module," *IBM Journal of Research and Development* 46, no. 6 (2002): 753-761.
- [11] Chow L.C., Ashraf N.S., Carter III H.C., Casey K., Corban S., Drost M.K., Gumm A.J., Hao Z., Hasan A.Q., Kapat J.S., Kramer L., Newton M., Sundaram K.B., Vaidya J., Wong C.C., Yerkes K., "Design and Analysis of a Meso-Scale

- Refrigerator," *Proceedings of the ASME International Mech. Eng. Congr. and Expos.*, ASME, 1999, p. 1-8.
- [12] Heydari A., "Miniature vapor compression refrigeration systems for active cooling of high performance computers," *Proceedings of the Inter Society Conference on Thermal Phenomena*, IEEE, 2002, p. 371-378.
- [13] Phelan P.E., Swanson J., Chiriac F., Chiriac V., "Designing a mesoscale vapor-compression refrigerator for cooling high-power microelectronics," *Proceedings of the Inter Society Conference on Thermal Phenomena*, IEEE, 2004, p. 218-23.
- [14] Mongia R., Masahiro K., DiStefano E., Barry J., Weibo C., Izenon M., Possamai F., Zimmermann A., Mochizuki M., "Small Scale Refrigeration System for Electronics Cooling within a Notebook Computer," IEEE, 2006, p. 751-758.
- [15] Chiriac V., Chiriac F., "An alternative method for the cooling of power microelectronics using classical refrigeration," *Proceedings of InterPACK*, ASME, July 17-22, 2005; San Francisco, CA.
- [16] Jeong S., "How difficult is it to make a micro refrigerator?" *International Journal of Refrigeration* 27 (2004): 309-313.
- [17] Tiedeman J.S., Sherif S.A., "Optimum coefficient of performance and exergetic efficiency of a two-stage vapour compression refrigeration system," *Proceedings of the Institution of Mechanical Engineers. Part C, Journal of Mechanical Engineering Science* 217, no. 9 (2003): 1027-1037.
- [18] Bhattacharyya S., Mukhopadhyay S., Kumar A., Khurana R.K., Sarkar J., "Optimization of a CO₂-C₃H₈ cascade system for refrigeration and heating," *International Journal of Refrigeration* 28 (2005): 1284-1292.
- [19] Kempaik M.J., Crawford R.R., "Three-zone, steady-state modeling of a mobile air-conditioning condenser," *ASHRAE Transactions* 98, no. 1 (1992): 475-488.
- [20] Ernst T., *Design, Fabrication and Testing of a Wearable Cooling System*, M.S. Thesis, Georgia Institute of Technology, 2005.
- [21] The Technical University of Denmark. "CoolPack Helpfiles." <http://www.et.web.mek.dtu.dk/Coolpack/UK/helpfiles.html>. Accessed March 2007.
- [22] Naeemi A., interview by author, Atlanta, GA, 8 May 2007.

- [23] Sözen A., Arcaklioglu E., Özalp M., "Calculation of thermodynamic properties of an alternative refrigerant (R508b) using artificial neural network," *Applied Thermal Engineering* 27 no. 2-3 (2007): 551-559.
- [24] Klein S.A., *Engineering Equation Solver*, (Middleton: F-Chart Software, 2006).
- [25] Patterson D.J., Brice C.W., Dougal R.A., Kovuri D., "The 'goodness' of small contemporary permanent magnet electric machines," *Proceedings of the International Electric Machines and Drives Conference*, 1-4 June 2003, IEEE, p.1195-200.
- [26] Kays W.M., London A.L., *Compact Heat Exchangers*, 3rd ed., (New York: McGraw-Hill, 1984), 270.
- [27] Incropera F.P., DeWitt D.P., *Fundamentals of Heat and Mass Transfer*. (Hoboken: John Wiley and Sons, Inc, 2002), 659-680.
- [28] Lee J., Mudawar I., "Two-phase flow in high-heat-flux micro-channel heat sink for refrigeration cooling applications: Part II – heat transfer characteristics," *International Journal of Heat and Mass Transfer* 48 (2005): 941-955.
- [29] Wadell R., Joshi Y., Fedorov A., "Experimental Investigation of Compact Evaporators for Ultra Low Temperature Refrigeration of Microprocessors," *Journal of Electronics Packaging*, in press (2007).
- [30] Collier J., Thome J., *Convective Boiling and Condensation*, 3rd ed, (Oxford: Clarendon Press, 1994), 466.
- [31] Bandhauer M., Agarwal A., Garimella S., "Measurement and Modeling of Condensation Heat Transfer Coefficients in Circular Microchannels," *Journal of Heat Transfer* 128 (2006): 1050-1059.
- [32] Coggins C., Gerlach D., Joshi Y., Fedorov A., "Compact, low temperature refrigeration of microprocessors," *Proceedings of the International Refrigeration and Air Conditioning Conference at Purdue*, July 17-20, 2006, West Lafayette, IN.
- [33] Bejan A., *Shape and Structure, from Engineering to Nature*, (New York: Cambridge University Press, 2000).
- [34] Sathe A., Lorenzo C., Groll E., Garimella S., "A New Model for an Electrostatically Actuated Miniature-Scale Diaphragm Compressor for Electronics Cooling,"

Proceedings of the International Refrigeration and Air Conditioning Conference at Purdue, July 17-20, 2006, West Lafayette, IN.

[35] Cabuz C., Herb W., Lu S., "The Dual Diaphragm Pump," IEEE (2001): 519-522.

[36] Norton R.L., *Machine Design*, (Upper Saddle River: Prentice-Hall, 1998), 540-541.

[37] Jähnig D.I., Reindl D.T., Klein S.A., A Semi-Empirical Method for Representing Domestic Refrigerator/Freezer Compressor Calorimeter Test Data, *ASHRAE Transactions* 106, no. 2 (2000).